Alpine gullies system evolution: Erosion drivers and control factors. Two examples from the western Italian Alps

Bollati I.M.[(1,*)], Masseroli A.[(1)], Mortara G.[(2)], Pelfini M.[(1)], Trombino L.[(1)]

Università degli Studi di Milano, Milano, Italia

Via Mangiagalli, 34 - 20133 Milan

irene.bollati@unimi.it

anna.masseroli@unimi.ti

manuela.pelfini@unimi.it

luca.trombino@unimi.it

(2) CNR –IRPI - Istituto di Ricerca per la Protezione Idrogeologica

Strada delle Cacce, 73 10135 – Torino

giovanni.mortara@irpi.cnr.it

(*) Corresponding Author: irene.bollati@unimi.it

Tel.: +390250315516

Fax: +390250315494

Abstract

Denudation processes affecting mountain slopes may vary according to different factors (e.g., lithology and structural setting of bedrock, climate, relief features), which may be very diverse at the local scale. Gully complex systems, characterised by morphological features similar to those developing in other climate contexts (i.e., pseudo-badlands) are also becoming common at higher altitudes and latitudes. The

selected study cases of Gran Gorgia (Susa Valley) and Saint Nicolas (Aosta Valley), in the Western Italian Alps, are sites of geomorphological interest as they are specifically relevant for their scientific features. The aims of this work are (i) reconstructing the morphometric evolution of gullies edges and vegetation colonisation in specific years by means of multitemporal spatial analysis on variation of surface areas affected by erosion; (ii) performing dendrogeomorphological analysis to spatially reconstruct, with a more continuous record through time, the effects of denudation processes affecting trees colonising the different regions of the gullies and the erosion rates by using dendrogeomorphological indicators (i.e., compression wood, traumatic resin ducts) and exposed roots and (iii) performing geopedological investigations aimed at deriving data on aggradation/degradation episodes along the slopes surrounding such hot-spots of erosion through time. Multidisciplinary analyses regarding the study sites allowed for detailing of erosional history of the studied slopes detecting the prevailing drivers of their evolution. According to the results and considering the common climate and bedrock conditions, the structural background seems to have more influence on slope evolution at the Saint Nicolas site, while superficial geomorphic processes seem to be more relevant at the Gran Gorgia site. Because the sites have already been recognised as part of geoheritage by local authorities, the data obtained in the present research on their genesis, evolution, and local drivers affecting the rates of denudation (i.e., scientific relevance of the site) suggests that description of the sites for dissemination purposes should include links to the entire slope history.

Keywords: gully systems; morphometry; dendrogeomorphology; geopedology; denudation rates; western Italian Alps

1. Introduction

Denudation processes affecting mountain slopes are variable in intensity according to different factors. Lithology and structural setting of bedrock (Cossart et al., 2013), as well as climate and relief features (Della Seta et al., 2009), are among the most efficient drivers and are very diversified at the local scale (Keiler et al., 2010).

In the context of mass wasting, gully systems are considered hot-spots of erosion in different morphoclimatic environments (Della Seta et al., 2009; Bollati et al., 2016a). The most studied cases are located in Mediterranean-like climate conditions, where dry periods are frequently followed by intense rainfall and where such sequence of meteorological conditions triggers the principal erosion events and contributes to the genesis of iconic landscapes (i.e., badlands like the Italian *calanchi* and *biancane*; Della Seta et al., 2009; Bollati et al., 2016b).

Morphological features similar to the badlands and gully systems developing in the Mediterranean climate are also becoming common at higher altitudes and latitudes (i.e., *pseudo-badlands sensu* Bollati et al., 2017). At higher altitudes, gullies mainly develop on loose glacial deposits, for example, on the inner flanks of lateral moraines, as a consequence of water runoff following deglaciation (e.g., Curry, 1999; Ballantyne, 2002; Cossart and Fort, 2008). This is a typical *paraglacial* readjustment affecting deglaciated areas, as described by Mercier et al. (2009). In polar environments, the *Index of gullying* on sediment mantled slopes has been in fact proposed by the authors for providing a time constraint to deglaciation in an area. According to Curry (1999) and Bollati et al. (2017), erosion rates affecting glacial deposits in mountain areas decrease proportionally to deglaciation time, proceeding

toward downvalley (Ballantyne, 2002), taking into account the local conditions (Cossart and Fort, 2008).

Besides progressive and continuous erosional work affecting mountain ranges at regional scale (e.g., Hinderer, 2001), locally the sudden evacuation of a huge amount of debris during single meteorological events can generate new landforms (Chiarle and Mortara, 2001). Extreme heavy rainfall events are becoming even more common within the ongoing climate conditions (Frei et al., 1998). After such perturbations (Ballantyne, 2002; Cossart and Fort, 2008), new landscape features may evolve under routine conditions recovering more regular erosion rates.

In addition to specific climatic and weather conditions, lithology and structural bedrock settings significantly contribute to the genesis of these erosional landforms, especially in tectonically active mountain ranges (e.g., *calanchi*; Farifteh and Soeters, 2006). Lithological and structural controls on the geomorphological dynamic along slopes play a key role at different spatial and time scales (Fort, 2000). Slopes characterised by tectonically deformed lithotypes present, as common features, deep-seated gravitational slope deformations (DSGSDs; Mortara and Sorzana, 1987). These DSGSD periodical reactivations may induce intensification of mass wasting and water erosion processes along the weaker portion of slopes (Mortara and Sorzana, 1987, and references therein). These deep deformations may severely affect the hydrographic patterns (Galeandro et al., 2013) until the complete obliteration of the stream network (Korup, 2005), inducing changes in water erosional patterns.

Iconic examples of gullies or overincision systems are locally evident in the Alpine range. Gully systems are locally characterised along their inner flanks by the development of, more or less pervasive, pseudo-badland features (Bollati et al., 2017; Fig. 1). As mentioned before, these deep gullies are sometimes consequent to single

extreme meteorological events, which have affected glacial deposits in more or less recent times (Mortara et al., 1995; Chiarle and Mortara, 2001; Chiarle et al., 2007). The gully systems in Alpine contexts can be grouped into three main categories, as used in this paper, according to the age of the deposits affected by rill erosion, to the rates of denudation, and finally, to the degree of vegetation colonisation. Gully systems developed on glacial deposits dating to the Little Ice Age (LIA) and, more frequently, to even more recent glacial stages (category 1; Fig. 1A) are reported as the most meaningful cases. Breaches may occur in moraines, and an impressive mass wasting (mainly debris flow) may occur, especially during extreme meteorological events. These landforms are usually still *fresh*, located at higher altitudes, not colonised by arboreal vegetation and characterised by incipient soils. Some examples for the Italian Alps are reported in the literature (e.g., Chiarle and Mortara, 2001; Chiarle et al., 2007): (i) the Sissone Glacier moraine system (Valmalenco; central Italian Alps) reworked by a disastrous event that occurred on 15 September 1950, with an estimated sediment delivery > 1 x 10^6 m^3 (Chiarle et al., 2007); (ii) the Mulinet Glacier moraine system (Valle di Lanzo, western Italian Alps; Fig. 1A) where the overincision of the moraine occurred on 29 September 1993, inducing an estimated sediment delivery of 0.8 x 10^6 m^3 (Mortara et al., 1995; Fig. 1A).

The second type of incisions affects older glacial deposits, related to upper Pleistocene. This typology is generally located at lower altitudes or several kilometres away from the current glacial snout position (category 2; Fig. 1C). In these cases, plant and tree colonisation of the bare surface is driven by both natural and human factors, soils are more developed and erosion rates are expected to be lower (Curry, 1999; Bollati et al., 2017). Some examples in the Italian Alps are represented by (i)

Saint Nicolas *calanchi* (Aosta Valley, western Italian Alps; Fig. 1C); ii) Neraissa Basins (Valle di Stura di Demonte, western Italian Alps).

Intermediate categories with transitional features between the two previous categories also exist (category 3; Fig. 1B) and an example is represented by the Gran Gorgia (Susa Valley, western Italian Alps; Fig. 1B).

Categories 2 and 3 are often located along the flank of the main Alpine valleys that underwent upper Pleistocene glacial modelling (e.g., Balteo Glacier for Saint Nicolas calanchi; Susa Glacier for Gran Gorgia). Following deglaciation, these valley slopes were locally affected by different postglacial processes such as decompression along preferential directions (e.g., debutressing; Cruden and Hu, 1993) according to local geological, structural and geomorphological conditions (e.g., DSGSDs); this may have different fallouts on the sediment cascade fluxes (McColl et al., 2012; Cossart et al., 2013).

The importance of such sites in understanding the post-glacial evolution of mountain landscapes, considering all the interplaying factors, opens the possibility of discussing the meaning of the most representative landforms like *geosites* or *sites of geological interest* (*sensu* Wimbledon, 1999). According to the definition by Wimbledon (1999), they represent key sites, characterised by a high scientific value, important for detecting the main stages of Earth system evolution. Moreover, gully systems are particularly meaningful from an educational point of view (Bollati et al., 2016a; Zgłobicki et al., 2017). They are *sites of geomorphological interest* or *geomorphosites* (*sensu* Panizza, 2001) and according to the classification proposed by Pelfini and Bollati (2014), they may be categorised as *active geomorphosites* or *evolving passive geomorphosites* depending on the type of the processes currently affecting the sites. In the first case, gully systems as geomorphosites are still evolving caused by their own

150 genetic process (i.e., badlands systems); in the second case, the processes inducing
151 morphological changes are different from the genetic ones (i.e., pseudo-badlands
152 superimposing on moraines). Hence, besides their scenic value that usually represents
153 the main motor for raising public interest, the scientific value of these landforms
154 should be central and requires even further investigations (Reynard et al., 2007;
155 Brilha, 2016).
156 If the events responsible for the genesis and/or for the morphological changes of
157 gullies in category 1 are well documented in the historical archives, less details are
158 available for categories 2 or 3 developed on older deposits (Chiarle and Mortara,
159 2001): so research on their evolution and respective drivers can be very important for
160 the reasons previously exposed. For this purpose, two sites were selected as study
161 cases: the Gran Gorgia (Fig. 1B; site A in Fig. 2) and the Saint Nicolas calanchi (Fig.
162 1C; sites B1 and B2 in Fig. 2).
163 Multidisciplinary approaches have been described in the literature (e.g., Mercier et al.,
164 2009; Burga et al., 2010; Compostella et al., 2013; Pelfini et al., 2014; Bollati et al.,
165 2016a; Eichel et al., 2016) as the best way to detect the contribution of multiple
166 factors (i.e., lithology and tectonic setting of bedrock, climate), which may drive
167 geomorphic processes like water erosion. A multidisciplinary approach could allow
168 for filling the gaps in the results obtained, operating using one kind of analysis to
169 confirm other deriving results.
170 In the present paper we aim at: (i) reconstructing the morphometric evolution of gully
171 systems and vegetation colonisation time by means of multitemporal spatial analysis
172 on surface morphological changes under water erosion; (ii) reconstructing in detail,
173 through dendrogeomorphological analysis, the progressive spatial surface denudation
174 and changes in erosion rates, by analysing trees and exposed roots and using different

indicators (i.e., compression wood, traumatic resin ducts); (iii) obtaining data on successive aggradation/degradation episodes along slopes surrounding such hotspots through geopedological investigations; and (iv) identifying which control factors exert a predominant role on denudation patterns in such contexts.

2. Study areas

The study sites are located in the western Italian Alps (Fig. 2) at the local altitude of the treeline ecotone. Their distinctive traits are described in the following sections. Both represent key sites for investigating gully erosion and for assessing their role as components of the regional geoheritage, as documented by their occurrence within local and national geosite catalogues.

2.1. Gran Gorgia (Susa Valley; Fig. 1B; site A in Fig. 2)

The Gran Gorgia gully (GG) is located on the northern side of the lower Susa Valley in the Chianocco Municipality (Turin Province). The slope is characterised by the outcrop of rocks belonging to two main tectonometamorphic units (Cadoppi et al., 2002). The Piedmont Zone (PZ) oceanic units and, locally, the *Val di Susa-Valle di Lanzo-Monte Orsiera tectonometamorphic unit* (SU), constitute the water divide between the Susa and Lanzo valleys. The main lithologies of the SU are serpentinites and serpenitoschists, prasinites, and metasedimentary rocks like calcschists. The SU overthrusts the *Dora-Maira tectonometamorphic unit* (DM), representing the Mesozoic continental margin units included in the Middle Penninic. Locally the dolomitic marbles of the Foresto-Chianocco-Mt. Molaras Complex constitutes the DM. The tectonic contact between SU and DM, marked by a very evident marble

bank, corresponds to the current head of the GG gully. According to Mortara (1975), the marble rocky outcrop may represent an obstacle for the regressive evolution of the gully.

The lithostructural control is relevant along the Susa Valley; and it is documented, especially on the southern side, by several DSGSDs (Cadoppi et al., 2007).

The GG gully develops NNW-SSE. It is located in the source area of the Prebec streams and it is incised in the upper Pleistocene glacial deposits (undistinguished till) pertinent to the tributary basin of the main valley, which is drained by the Dora Riparia and shaped, in ancient times, by the Susa Glacier (Sacco, 1921; Cadoppi et al., 2002; Ivy-Ochs et al., 2018). The Dora Riparia Valley outlet, near the town of Torino and about 40 km away from the GG area, is characterised by the presence of the Rivoli-Avigliana morainic amphitheatre, one of the most important and intact witnesses of the Pleistocene glacial advances as far as the Po Plain (Lucchesi et al., 2015; Giardino et al., 2017; Ivy-Ochs et al., 2018). The glacial deposits related to the Prebec tributary basin span between 1000 and 1850 m asl (Cadoppi et al., 2002). At this altitude tributary glaciers flow into the main glacial basin belonging to the Susa Valley. The slopes surrounding the GG gully are currently affected by water and gravity-related processes (rock degradation and falls, landslides and debris flows) and by snow avalanches with the associated deposits. Locally, elongated ridges are present, interpreted by Sacco (1921) as deriving from ice-snow field deposits and, more recently, related with combined snow and gravity activity (Cadoppi et al., 2002).

The GG is characterised by an asymmetric shape with the eastern slope longer and less steep, with a more elevated upper edge than the western one. Inner slopes are characterised by parallel linear ridges and gullies. The scarp edges are irregular, according to the prevailing geomorphic process: (i) water runoff where slope

steepness is lower and (ii) debris fall (i.e., coarse boulder) where steepness increases until the vertical. The eastern edge is interrupted by a breach generated by regressive erosion acting on the western slope of the eastward adjacent valley.

The genesis of the GG, whose presence has been slightly perceptible at least since the early twentieth century on historical topographic maps, was hypothesised to be related with a single extreme meteorological event that occurred during the fifteenth century (Regione Piemonte, 1995). The hypothesis is supported by the morphological analogies with the breach in the Mulinet Glacier moraine in 1993 (Fig. 1, A; Chiarle and Mortara, 2001). The volume of eroded sediment during the single event is about 1.5×10^6 m^3 (Aigotti et al., 2004).

According to Mortara (1975), the Prebec basin has undergone an average of 1600 flood events during the last 10,000 years. The author estimated a total amount of 80×10^6 m^3 of delivered sediment, representing almost the totality of the volume of the alluvial fan on which the Chianocco village is built. Several recent hydrogeological instability events affected the Prebec basin (e.g., June 1957, August 1977 and 1978, November 1994, October 2000, August 2002; Tropeano et al., 1999, 2006). A debris mass of 0.05×10^6 m^3 was deposited on the Chianocco alluvial fan during one of the most disastrous events that occurred on 12-16 June 1957 (Mortara, 1975). In other cases, the debris floods also affected touristic infrastructures (camping), as on 14 August 1978 (Mortara and Turitto, 1989). If several damages affected the village and the surrounding areas in the historical records of events, many human interventions also stabilised the stream (i.e., weirs) and the adjacent slopes (i.e., reforestation) (Anselmo et al., 1975; Mortara, 1975).

In this area, as a consequence of slope steepness and of the presence of surficial erosion caused by water-driven processes, only soils rich in coarse material and

poorly developed and only in a few cases with a surface layer rich in organic matter are present. In fact, Entisols and Inceptisols are the most common soil types in the GG study area (Carta dei Suoli del Piemonte, 1:25.000; IPLA, 2007).

Concerning climate, the Susa Valley, elongated in the E-W direction, is one of the most drought-affected valleys of the western Italian Alps (De Luca et al., 2009), similar to the climate of the Italian southern Alps region. According to the data from the Prarotto weather station (1440 m asl) (Arpa Piemonte, http://www.arpa.piemonte.gov.it/), local climate conditions, related to the period 1998-2014 (excluding the years 2004, 2006, and 2013), are characterised by mean annual rainfalls of 848 mm. Mean annual temperatures for the period 1998-2017 (excluding the years 2004, 2013, and 2014) vary between the minimum average values recorded in January (-0.1°C) and the maximum average values recorded in July (15.9°C). The temperature annual range at 1440 m a.s.l is ~ 16°C.

The site has relations with the Rivoli-Avigliana morainic amphitheatre geosite (Lucchesi et al., 2015; Giardino et al., 2017) and is located on a slope along the Susa Valley. In addition, Giordano et al. (2016) reconsidered the Franks trail, developing along the Susa Valley and along which the site is located, as a cultural-geological path. Moreover, the site is inserted in the list of geosites of Turin Province (Aigotti et al., 2004) and is reported in the ISPRA national geosites inventory (http://sgi.isprambiente.it/geositiweb/scheda_geosito.aspx?id_geosito_x=1439).

2.2. Saint Nicolas calanchi (Aosta Valley; Fig. 1C; sites B1 and B2, Fig. 2)

The Saint Nicolas calanchi (SN) is a gully incision developing mainly NNW-SSE and located on the northern side of the Aosta Valley in the Saint Nicolas municipality (Aosta Province). The slope hosting the site is characterised by the presence of

tectonometamorphic units pertaining to continental and oceanic domains (Polino et al., 2015). The slope is affected by the presence of the relevant DSGSD of Punta Leysser (Forno et al., 2012), whose limits roughly correspond to the tectonic contacts between structural units. In detail, the western and northern edge of the DSGSD are characterised by the *Gran San Bernardo multinappe system*, included in the Middle Pennidic domain, which is constituted by the Palaeozoic continental units of *Rutor* (paragneiss and micaschists with prealpine relicts) and *Fallère-Metailler* (micaschists, paragneiss, and metabasites). The central portion of the slope, where the greatest part of the DSGSD is located, is dominated by the Mesozoic *Aouilletta ophiolitic unit* (undistinguished calcschists, metabasites and prasinitic gneiss, serpentinites and oficarbonates with local marble), representing a portion of the Piedmont Zone separated from the Penninic units by the *Inner Houillere Front*. Locally, along the slope, the shear and faulted zones are marked by carbonate-cemented breccia.

As mentioned before, the morphology of the slope is mainly affected by the activity of the Punta Leysser DSGSD that produces typical traits such as trenches, counterscarps, and double or multiple ridges. A particular feature is constituted by the presence of travertines locally outcropping and related to water infiltration caused by the DSGSD dynamics (Forno et al., 2016). According to Forno et al. (2013, 2016) and Pini et al. (2013), the preservation of Quaternary deposits is favoured in such areas by the irregularities of the slope, mainly elongated ridges, which favour deposition. These areas, where deposition prevails, alternate with areas prone to erosion, especially along the hydrographic network, whose pattern is driven by the structures. The Quaternary sedimentation is, for the authors, strictly dependent from the structural setting.

The site is located along the northern side of the main glacial Aosta Valley shaped by the Balteo Glacier, which was fed locally by tributary glaciers (i.e., Clusellaz, Verrogne, Gaboè, and Vetan; Forno et al., 2012). The witnesses of their presence, besides the related deposits, are mainly glacial cirques, aretes, and rôche moutonnée, as well as overdeepenings and depressions that interplay with the structurally derived ones. Besides, the study site is located along the northern slope bordering the *Conca di Aosta*, where an overdeepening was generated by the interaction between the gravitational deformation and the Balteo Glacier action, allowing for the formation and deposition of a great quantity of debris. Along the investigated slope, the *Ivrea Synthem* deposits represent the witness of the last glaciation that reached the position of the Ivrea morainic amphitheatre about 90 km downstream (Fig. 2) (Gianotti et al., 2015). This represented, as did the Rivoli-Avigliana morainic amphitheatre, a significant witness of the Pleistocene glacial advances (Lucchesi et al., 2015; Giardino et al., 2017). Locally, during the Last Glacial Maximum (29-19 ky BP; Gianotti et al., 2015), the Balteo Glacier reached a maximum altitude of 1800 m asl (Sacco, 1927; Forno et al., 2012). In the area, within the Ivrea Synthem, the *Colle San Carlo* and the *Excenex Subsynthems* are reported (upper Pleistocene; Polino et al., 2015). The first one, constituted mainly by undistinguished till, characterises higher altitudes (as far as about 2000 m asl); while the second one, essentially made by locally stratified lodgement till, occupies the lower portion of the slope (as far as about 1500 m asl). Another more recent Subsynthem, included in the Ivrea Synthem and characterising the study area, is the *Pileo Subsynthem* related to the Lateglacial stage (Upper Pleistocene - Lower Holocene; Polino et al., 2015). In the study area, its deposits cover the upper portion of the slope (above 2000 m asl) and are interpreted as lodgement till (Polino et al., 2015). Only near the Mont Fallère water divide, where

the glacial cirques are present, the very recent postglacial deposits, belonging to the *Miage Synthem* (Holocene - Present), are described in the literature. Besides the glacial deposits, gravity related deposits are also present.

Gullies represent a common feature along the slope, where the cutting of glacial deposits is more evident. Gullies are more articulated and mature along the Gaboè and the Montovret streams, respectively draining the geosite (at about 2000 m asl; site B1 in Fig. 2) and the calanchi area located to the south of Rumiod village (at about 1200 m asl, 3.5 km southeasterly of the geosite, site B2 in Fig. 2), while the gullies are incipient in other cases. The locations of the gullies are driven by gravitational morphostructures (e.g., longitudinal trenches; Forno et al., 2012). The SN geosite develops upward to an abrupt westward diversion of the DSGSD western edge, along the Gaboè stream. The Montovret site presents a one-sided pseudo-badlands slope, west oriented, located in the core of the DSGSD. Measurements of erosion were performed along the Gaboè and the Montovret gullied stream sites in the present research. The SN is characterised by irregular scarp edges where water runoff or gravity may prevail; and it is divided into subbasins, some of which are characterised by typical badlands in a different respect to the GG site. In particular, the eastern slope is more affected by gullying processes; and along the eastern scarp edge, more inward with respect to the DSGSD western edge, they assume the typical morphology of a ‘rather small hydrographic unit, horse-shoe shaped, with a tributary system in which each channel is separated from the adjacent ones by means of more or less sharp ridges’ (Alexander, 1980). The western edge is more regular and similar to the GG, characterised by parallel ridges alternating to gullies, and is transversal with respect to the main gully.

Human interventions realised in the middle of the twentieth century were addressed to slow down regressive erosion by means of a series of weirs located along the Gaboè stream and of reforestation practices and artificial terracing (source Regione Valle D'Aosta).

The study area of SN is characterised by different types of soil (Carta Ecopedologica d'Italia 1:250.000, 2013; http://wms.pcn.minambiente.it/ogc?map=/ms_ogc/WMS_v1.3/Vettoriali/Carta_ecopedologica.map). At higher altitude, thin soils (Leptosol) and soils characterised by a surface layer rich in humus (Umbrisol) were mapped. Whereas, at lower altitude the slope is mainly characterised by very thin and not well developed soils (Leptosol, Regosol), the more stable areas are characterised by soils with weak horizon differentiation, and is highlighted by changes in physical and chemical properties like colour, structures or clay content (Cambisols).

The climate in this portion of the Aosta Valley, as in the Susa Valley elongated in the E-W direction, has a semicontinental temperature regime with an annual temperature range of about 20°C. Rainfall is scarce (about 680 mm in the main valley), with 70% of the land receiving < 1000 mm/y (Mercalli et al., 2003). Considering the meteorological trends recorded during the period 1995-2012 in Aosta (Saint Christophe meteorological station; Arpa Valle d'Aosta, http://cf.regione.vda.it/ufficio_idrografico.php), on average precipitation is are concentrated in autumn and spring, with a minimum recorded during winter (531 mm annually). Concerning temperature, the winter minimum average temperature is in January (-0.4°C), and the summer maximum average temperature is in July (21.7°C), with an annual thermal excursion slightly over 20°C.

372 The site is a geosite of the Aosta Valley
373 (http://www.regione.vda.it/territorio/territorio/geositi/snicolas/default_i.asp) that the
374 municipality of Saint Nicolas decided to enhance by means of a geotouristic trail
375 linking Gaboè and the Montovret calanchi sites (http://www.comune.saint-
376 nicolas.ao.it/index.php?option=com_contentandview=articleandid=183andItemid=10
377 9).
378
379 **3. Materials and methods**
380 *3.1. Multitemporal analysis of gully surface changes caused by water and gravity*
381 *erosion*
382 The multitemporal mapping of the bare surfaces affected by water runoff (i.e.,
383 surfaces with scattered vegetation and not characterised by soil development) was
384 performed in a GIS environment (ESRI software ArcGis 10.2.1, ArcMap) using a
385 series of orthophotos available only as a GIS server of the National Web Map Service
386 (i.e., Geoportale Nazionale, WMS Service; http://wms.pcn.minambiente.it/).
387 Considering this source data, with a resolution of 0.5 m, the expected error is of ±2%
388 (see Smiraglia et al., 2015). The orthophotos date respectively to 1989 (GG) / 1988
389 (SN); 1997 (GG and SN); 1998 (GG) / 1999 (SN); 2007 (GG) / 2006 (SN), 2012 (GG
390 and SN). After mapping the areas, percentages of surface variations during the entire
391 investigated periods were calculated with respect to the initial surface area size (i.e.,
392 1988 for SN and 1989 for GG), and the percentage of changes was also calculated for
393 each time subinterval. Additional morphometric features were derived for the GG
394 from the DTM (10 m; Regione Piemonte, http://www.geoportale.piemonte.it/cms/;
395 1997-2008) and for SN from the DTM (2 m; Regione Valle D'Aosta,
396 http://geoportale.regione.vda.it/; 2005-2008).

3.2. Dendrogeomorphological analysis

Erosion caused by water runoff and slope processes (e.g., mass wasting events, snow avalanches) have been investigated by means of dendrogeomorphological analyses, techniques widely applied to detect, discriminate, and date geomorphic events affecting trees colonising landforms (e.g., Alestalo, 1971; Guida et al., 2008; Pelfini and Santilli, 2008; Stoffel and Bollschweiler, 2008).

In order to detect the geomorphic dynamics affecting the investigated sites and the surrounding slopes, field surveys were carried out during 2013, 2015, and 2016. The sampling design was established by grouping trees into subclusters ideally characterised by different geomorphic dynamics and located at a progressive distance from the main gully. At tree sample sites, analyses of the soil profiles were also performed, where possible (see section 3.3).

In the GG case, 86 trees of *Larix decidua* Mill. were sampled belonging to the five sub-clusters reported, in relation with soil sampling in Table 1. The total number of sampled trees is 61 for the A1-A5 subclusters and 25 for the A6-A7 subclusters.

Along the SN slope, a similar procedure was followed. Two main sites and relative subclusters were selected: the SN site along the Gaboè stream (B1) and the Rumiod site along the Montovret stream (B2) (Table 1). The total number of sampled trees of *Larix decidua* Mill. species is 30 for the B1.1-B1.4 subclusters and 15 for the B1.5 subcluster. Moreover, in the B2 area 13 trees of *Larix decidua* Mill. and 4 of *Pinus sylvestris* L. located along the scarp edge were analysed. In both sites, a cluster of undisturbed trees (at least 15 trees) was selected to build the reference chronologies to be used to discriminate regional or local origin of the disturbances.

421 Concerning samples from the trunk, the specimens were extracted using a Pressler
422 increment borer. At least two samples in different positions for each tree were
423 extracted taking care of sampling for one core to investigate the disturbance
424 specifically (e.g., scars, tilted portion of the stem) (Stoffel and Bollschweiler, 2008).
425 Concerning the undisturbed specimens, especially those for building the reference
426 chronology, they were extracted at a standard height of 1.30 m (breast height). In
427 order to analyse root micromorphology, disks were cut using a saw.
428 After the first phase of microscopic analysis using the LINTAB system (Rinn, 1996),
429 tree ring widths were measured (accuracy of 0.01 mm) according to the features of the
430 specimen using the Lintab and TSAP systems (Rinn, 1996) and/or by means of image
431 analysis performed with WinDENDRO software (Régent Instruments Inc., 2001). The
432 mean chronologies for the disturbed and undisturbed clusters of trees were elaborated
433 by means of the cross-dating procedure with TSAP and COFECHA (Holmes et al.,
434 1986). Moreover, in order to remove growth trend, a detrending was performed by
435 means of a spline function, using Arstan (Holmes et al., 1986). Afterward, the dating
436 of each individual annual ring, and consequently disturbance, and the determination
437 of the age of geomorphic events, was possible.
438 In order to perform erosion rate estimation by means of exposed tree roots, roots were
439 the object of microscopic morphometric analysis and measurement using Lintab and
440 TSAP systems (Rinn, 1996). Roots change their micromorphology, from the
441 production of root type wood to a trunk type wood as a consequence of exposure
442 (Gärtner, 2007; Stoffel et al., 2013) (Fig. 3). According to this response of roots, the
443 erosion rates were calculated starting from the equation proposed by Hupp and Carey
444 (1990):
445 $$E = D/A \quad (1)$$

The formula allows for obtaining the erosion rate by dividing the distance *D* between the tree root top and the actual ground surface by the age *A* of the micromorphology change in root. Because samplings were performed during the summer months, a variable portion of the sampling year (*Year Fraction; YF*) should be added to the *A* parameter for reducing the overestimation of the erosion rate. Hence, the herein applied formula was

$$E = D/(A+YF) \quad (2)$$

where

$$YF = (1/12) * N° \, month \quad (3)$$

where *N° month* represents the progressive number of the month within a year (e.g., July = 7; $YF_{July} = 0.583$).

Considering that roots from the same tree might be exposed in different times, *Local Erosion Rates (LERs)* at single tree root sample and *Average Erosion Rates (AERs)* over long periods in the extended areas (e.g., Bollati et al., 2016a, b) were finally obtained.

Besides erosion rates, attention was also paid to the most commonly used dendrogeomorphological indicators for detecting geomorphic disturbance by processes that may trigger erosion (e.g., mass wasting, snow avalanches). These processes in fact may interact with water runoff altering the normal erosion values (Bollati et al., 2016a). The *Compression Wood* (*CW*) is a particular, resistant, and denser kind of wood produced by the tree in response to mechanical stress induced by the tilting of the stem (Fig. 3) caused mainly to creep or other destabilising processes (e.g., Timell, 1986; Bollati et al., 2018). *Traumatic Resin Ducts* (TRDs) are aligned resin ducts, which are specific features that may be produced in trunks affected by traumas deriving from the impact of material caused by geomorphic processes

inducing debris transport (e.g., snow avalanches, debris flows, rock falls) (e.g., Bollschweiler et al., 2008; Garavaglia and Pelfini, 2011). Because TRDs are produced immediately after the stress, they have already been used to date and to discriminate geomorphic processes with a seasonal resolution according to the location of the ducts within the early- or latewood (e.g., Kogelnig-Mayer et al., 2011; Bollati et al., 2018). According to Kogelnig-Mayer et al. (2011), TRDs located within the latewood may indicate, more probably, damages from mass wasting (e.g., debris flows, landslides), which are more frequent during late summer until early autumn; instead TRDs characterising earlywood may indicate, more probably, damages from winter/spring snow avalanches.

3.3. Geopedological sampling and analysis

Soil profiles were chosen for sampling, where possible, in correspondence with specific geomorphic conditions and of dendrogeomorphological sample sites, as described in Table 1. In both study areas, soil profiles were selected (i) along the slope, in order to observe the slope dynamics; (ii) on the edge of gullies, in order to understand the erosion dynamic under water-driven processes; and (iii) in flat and/or stable areas (i.e., undisturbed in Table 1) in order to observe soil development in a steadier geomorphological context. All the profiles were dug taking advantage of the presence of a natural scarp, except for profile SN16/02 where a digger was used. Each soil sample was then subjected to routine laboratory analysis to determine particle size distribution, pH (in 1:2.5 soil:distilled water) and organic carbon content (Walkley-Black method) (Ministero delle Risorse Agricole Alimentari e Forestali, 1994).

In regards to the grain - size analyses, air-dried soil samples were treated by wet sieving in order to separate skeleton particles from the fine earth. For what concerns

fine earth, after a pre-treatment of the samples with H_2O_2 (130 volumes), particle size distribution was determined by a combined method consisting of sieving the sand particles (1400–63 μm) and measurement of the silt and clay particles (<63 μm) by aerometry, with the method of the Casagrande aerometer.

4. Results

4.1. Multitemporal analysis of gully surface changes caused by water and gravity erosion

Concerning the GG site, the main morphometric features are reported in Table 2. The site is quite regularly developed all along its length, but the western edge is less elevated than the eastern edge. The highest difference value (42 m; Table 1) is recorded in the area where the interruption of the eastern edge by the regressive erosion of the external slope occurs.

The multitemporal analysis of surface area changes caused by water runoff indicates a general trend of decreasing bare surface areas (Fig. 4, A; Table 1). The percentages of variations with respect to the initial surface area during the 1989-2007 time interval never exceeded 1%. A slight increase (<0.12%) of bare surface is recorded only during the 2007-2012 period. The mapped areas are reported in Fig. 3 as well as the percentage of surface variations, averaged over their respective time interval.

Concerning the SN site, water runoff does not homogeneously interest the surface along the main gully, whose width is variable. Three main subsectors can be recognised according to morphometric and gully width observations and measurements (see Table 2):

- the main gully is narrower and the edges are regular in the uppermost portion;

- the main gully is becoming wider and is characterised by a more continuous vegetation coverage on the western side in the central portion; the development of five main *horse-shoe shaped* calanchi basins is evident on the eastern side in the central portion (Fig. 4, B); this sector presents an asymmetric transversal section with a significant difference in altitude between the two scarp edges (60 m; Table 1); and
- the last trait is more irregular and asymmetric, as well as well colonised by vegetation and it represents the closure section of the gully.

The width variations of the surfaces affected by water runoff at the SN, in the 1988-2006 time interval, is represented by a decrease between 0.11% and 2.46%, accompanied by an increment of vegetation along the calanchi slopes.

4.2. Dendrogeomorphological analysis

Concerning trees colonising the surfaces of the GG site, the oldest tree (58 years minimum age) is located along the slope, immediately west of the GG. About half of the trees (40% not considering the trees in the forestry conditions A6 and A7) are 30-40 years old minimum and colonise the slope (mainly A1, A2). Trees belonging to the transects (A5), first mapped in the 2007 orthophoto along the lateral slope of the gully (A5), are younger than 30 years and, more frequently, are <20 years old.

Trees with exposed roots are mainly located along the GG scarp edge (A3, A4). The LERs are variable between trees and within the same tree. Along the upper scarp edge (A3), the maximum LER value is 30.57 cm/y, in correspondence with local debris fall. The AER, considering the beginning of the exposure and excluding the minimum and maximum values, is 2.81 cm/y. Also along the slope immediately behind the scarp edge, surface erosion denudates tree roots (Fig. 5). Here, the AER in

546 correspondence with the only tree with exposed roots is 0.87 cm/y. The older ages of
547 exposure (1986-2002) are recorded in the lower portion of the scarp (A4). The most
548 recent exposures occur in the upper portion of the scarp (A3), where the maximum
549 LERs have also been calculated.
550 Considering the higher number of trees during recent years, the years with the greatest
551 number of trees characterised by TRDs are 2003 and 2006 followed by 2004, 2007,
552 and 2010 (Fig. 6). During these years, the groups more affected by earlywood and
553 latewood TRDs are A3 and A4. The TRDs in the earlywood are more homogeneously
554 distributed in time and space, particularly along the scarp edge in 2006 and 2007. The
555 latewood TRDs affected A3 trees in 1985, 1990-1992, 1995, and 2008 and affected
556 A5 trees especially in the 2002-2004 time interval.
557 Concerning CW at the GG site, the trend is quite discontinuous. The trees mainly
558 affected are those belonging to the A3 and A4, located on the slope immediately west
559 of the scarp edge and interested continuatively by instability. During the second half
560 of the 1990s of the twentieth century, the CW propagated to the slope trees (A1 and
561 A2).
562 The transects inside the gully (A5) are characterised by abundant CW even if this data
563 should be handled with care as these trees have recently germinated and their young
564 and elastic trunks may be more prone to destabilisation. In general, trees located along
565 the edge are undermined by the instability of the substrate inside the gully, as local
566 falls also involve (besides debris) trees (between 2013 and 2016 evident changes were
567 recorded). The CW is found related, on the inner western slope, to creep and
568 instability induced by the high steepness of the slope itself and of the bottom of the
569 gully.

570 Moving to the SN site, tree vegetation in the Gaboè (B1) and in the Montovert area
571 (B2) has been colonising surfaces for a long time but with some differences. The
572 oldest trees were dated to the beginning of the twentieth century by cross-dating mean
573 chronologies from each tree with the reference chronologies; they are located in the
574 western inner part of the geosite (B1.4) and up to the geosite (B1.2) (Fig. 5, B). Trees
575 are not older than 1989 near the bottom of the gully (B1.4), while along the western
576 scarp (B1.3) the oldest tree dated back to 1930. At the B2 site vegetation dated back at
577 least to the end of the 1960s of the twentieth century.
578 Exposed roots were observed and LERs were calculated at the B1.3 (the western scarp
579 edge at the geosite) and at the B2 (Fig. 5, B). In the B1.3 site LERs span between 0.29
580 and 3.01 cm/y. The spatial AER along the scarp edge (B1.3) is 1.38 cm/y. The years
581 of exposure span between 1958 and 2013. In B1.2, located along the Gaboè stream up
582 above the geosite, the LER is 0.29 cm/y. The B2 is characterised by LERs, which are
583 lower between 0.08 and 1.40 cm/y. Exposure years span between 1981 and 2014, and
584 the spatial AER for this period is 0.84 cm/y.
585 The TRD distribution is quite inhomogeneous and less representative than in the GG
586 site. The TRDs are present in B1 during different years within trees. The B1.3 and
587 B1.4 are the subclusters most affected by TRD occurrence. More than one tree is
588 affected by TRDs only during 1999/2000 and 2003/2004. The B1.1 trees in one site
589 present TRDs in 2004/2005. The B2 tree data coincides with the other sites for TRDs
590 only in 2000 and 2004/2005.
591 The CW does not show precise trends and is not abundant as expected. The CW is
592 more frequent in B1.4: in the bottom of the gully and on the eastern slope it is
593 recorded during the period 1990-2005; on the other side it was present before the

1990s. An overlapping time interval characterised by CW was also observed for subsites: 1997-2004 for B1.1; 1992-2002 for B2.

4.3. Geopedological analysis

The analysed soil profiles at the GG site show a weak degree of development and an unmarked horizon differentiation, except for the soil profile located at the edge of the main gully (P04) and for the soil profile used as a reference and located in the forest (P06).

Indeed, soil profiles show thickness <1 m; they are characterised by a moderately expressed soil structure and by granular or subangular blocky aggregates. The colour, in dry condition, is quite homogeneous in overall horizons and profiles (characterised by a hue rarely different from 2.5Y).

All soil profiles have a considerable skeleton content (material >2 mm), and gravel is very abundant with peaks over 50% in some horizons (Fig. 7). Gravel content is <10% only in the surficial horizons. In regards to the fine earth, sand is the most represented fraction, which ranges between 17 and 42.6% of the total weight; whereas the less represented grain size fraction is clay, which rarely exceeds 20% of the total weight (Fig. 7).

Moreover, grain size distribution cumulative curves (Appendix 1a) show a low degree of selection with a predominant sand presence, except for profiles located in more stable areas (P06 and P08) and for the profile located at the edge of the gully (P04). Generally, the percentages of gravel and sand increase along the profile to the detriment of silt and clay components (Fig. 7). Instead, in profile P07 a little grain size trend anomaly is found: horizon C2 is characterised by a sand, silt, and clay content

618 increase accompanied by a decrease of gravel content when compared to the above
619 horizon (Fig. 7).
620 A decreasing trend with depth of organic carbon is observed in all soil profiles. The
621 absolute quantity of organic carbon varies between 4.1 and 164 g/Kg (Fig. 7).
622 Horizons within the soil profiles have pH values ranging from 5.5 to 7.4 (Fig. 7).
623 Generally, the superficial horizons are more acid, in particular in P03 and P08.
624 The soil profiles studied by geopedological analysis at the SN site (B1), located in a
625 flat and more stable area (SNA16/02; SNA16/03), are more developed and thick when
626 compared to the profiles placed at the edge of gully (SNA16/01 and SN03) or on the
627 slopes (SN01 and SN05). Soil structure is moderately developed and is mainly
628 characterised by granular or subangular blocky aggregates.
629 Particle size distribution in the analysed soil profiles shows that gravel and sand are
630 the most represented grain size fractions (Fig. 8); in fact, sand content varies between
631 16 and 57.4%, and the content of gravel varies between 6.6 and 79.2%. Silt quantity is
632 more variable, instead clay is limited and always below 10% in total weight.
633 Grain size decreases in SN05 and SNA16/03 from the parent material to the surface
634 soil horizons, where the highest clay and silt contents are found.
635 Instead, in SN01, in the deepest horizon 2A there is an increase of silt and clay
636 contents compared to the above horizon. Moreover, the gravel content decreases
637 along the profile, whereas the sand quantity remains roughly constant (Fig. 8).
638 A grain size trend anomaly is also found in SN03, where sand, silt, and clay contents
639 increase in the 2AC horizon, accompanied by a decrease of gravel when compared to
640 the above horizon (Fig. 8).
641 Silt and clay content decreases along the profiles in SNA16/01 and SNA16/02. The
642 coarse material tends to increase, but the superficial horizon shows higher gravel

643 content compared to the below horizon. Moreover, observing the cumulative curves
644 of SNA16/02 grain size distribution (Appendix 1b), the superficial AC horizon shows
645 a very different trend from other horizons. The cumulative curves show a low degree
646 of selection, with a predominant sand presence, except for profiles located in more
647 stable areas (SNA16/02 and SNA16/03).
648 The absolute quantities of organic carbon vary between 3.4 and 101.1 g/Kg (Fig. 8).
649 The organic C values decrease with depth in all the analysed profiles except for SN01
650 and SN03, where the superficial horizon does not have the highest quantities of
651 organic C.
652 In particular, in SN01 the peak of organic C is in the deepest horizon (2A), while in
653 SN03 the organic C content shows a peak in the 2AC horizon (Fig. 8).
654 In all horizons of the analysed soil profiles, the pH values range from 4.1 to 8.1 (Fig.
655 8). On average, the surficial horizons are more acid, in particular in SNA16/02 and
656 SNA16/03. More or less in all profiles the pH increases along the profile, approaching
657 the parent material.
658
659 **5. Discussion**
660
661 The results obtained in the two study cases allow us for making some remarks on the
662 reliability of applying a multidisciplinary approach to reconstruct slope evolution in
663 relation to geomorphic processes and/or structural setting conditioning on erosion.
664 A summary of the findings at GG and SN is reported in Table 3, where the main
665 indicators of disturbance in both sites are listed.
666 On one side, the sites are very similar concerning climate conditions and bedrock. In
667 the first case, both sites are located along the south-facing slope of a main E-W

668 oriented valley, in which climate regime presents a trend characterised by marked
669 drought periods alternating with wet periods, and extreme rainfall events are even
670 more frequent (Frei et al., 1998). This, as in other climate contexts (i.e.,
671 Mediterranean; Della Seta et al., 2009), favours water-related erosion, especially if
672 loose deposits are outcropping. These conditions are also common in other localities
673 where similar measurements on erosion of glacial deposits were performed with the
674 same methodology (e.g., Pyramides d'Euseigne, Valais Canton, Switzerland; Bollati
675 et al., 2017), resulting in lower AERs (0.58 cm/y; Bollati et al., 2017; see discussion
676 after).
677 The sites also present similar bedrocks and, consequently, parent materials as a
678 relevant abundance of ultramafic and calcareous debris was surveyed.
679 Moreover, the multitemporal measurements of the areas affected by erosion allow us
680 for discovering a similar trend between sites. Both sites are characterised by a general
681 reduction of surfaces affected by water runoff, except for the most recent times during
682 which a slight increase was detected at the GG site (0.1%; 2007-2012). All values,
683 considering the possible error using the WMS source, fall within the percentage (i.e.,
684 2%), except for the SN site where during the 1988-1997 time interval the bare surface
685 shows a decrease slightly greater than the plausible error 2% (i.e., 2.46%). Hence, the
686 increase of bare surface could not be interpreted as a significant increase of the areas
687 affected by erosion as expected by other authors (Mortara, 1975).
688 Anyway, in both sites, the maximum LERs have been calculated along the edge of the
689 main gully (30.57 cm/y at GG and 3.01 cm/y at SN). At GG lower values were
690 calculated on the slope surrounding the gully. At SN, even more significant, the AER
691 at B1 (1.32 cm/y, excluding the minimum and maximum values), located along the
692 Punta Leysser DSGSD edge, is greater than AER at B2 (0.90 cm/y, excluding the

693 minimum and maximum values), located on the main DSGSD body.
694 Dendrochronological analysis of trees sited along the GG scarp edge shows how the
695 area is locally characterised by debris falls: damaged trees are present in
696 correspondence with the highest values of erosion calculated by means of tree root
697 exposure. This may suggest a more intense deepening of the thalweg that may favour
698 scarp instability. Also at the SN site (B1), local instabilities should be taken into
699 account as documented by ages of trees growing near the bottom of the gully, which
700 were younger (germination year after 1989) and more disturbed.
701 If the surface analysis does not reflect the very local changes along the edges, further
702 multitemporal laser scanner analyses, aimed at detecting variations of the gullies
703 morphology, may be helpful (e.g., Cossart and Fort, 2008).
704 Some significant differences were detected between the sites combining
705 dendrogeomorphological and geopedological results.
706 The more evident difference between the SN and GG sites was detected concerning
707 the recurrence and frequency of the dendrogeomorphological indicators (CW and
708 TRDs). In the GG sites, CW and TRDs are recurrent and provide useful information
709 on the different types of geomorphic events related to surface processes (such as snow
710 avalanches and debris flows), but in SN neither CW nor TRD significant trends were
711 observed. This could be related to the difference in the intensity of surface processes
712 affecting the two investigated slopes. While GG is located along a very steep slope
713 (average steepness at the bottom of the gully is 48%, Table 1) where avalanches are
714 common and vegetation colonises the inner part of the gully with difficulty, SN is
715 located in a less steep area (average steepness at the bottom of the gully is 28.7%,
716 Table 1), being more protected from the geomorphic processes, where vegetation is
717 older and also human impact has been more significant (e.g., reforestation of slopes,

718 human settlements since ancient time in the area). These results suggest one should
719 expect different information coming from dendrogeomorphological indicators
720 according to site local features (e.g., Garavaglia and Pelfini, 2011).
721 Another dissimilarity between sites is related to the maximum LERs that are very
722 different: 30.57 cm/y in the upper portion of the western scarp edge at GG (A3) and
723 3.01 cm/y along the western scarp edge of SN (B1.3).
724 Concerning geopedological results, in the studied soil profiles at GG and SN study
725 sites, the analysis of particle size distribution underlines the preponderant presence of
726 coarse material typical of mountain weakly developed soils. Moreover, the influence
727 of parent material on soil features is also evident taking into consideration the pH
728 analysis, which shows a neutral to slightly alkaline pH in all profiles. Only soil
729 profiles located in stable and flat areas, in the forest (i.e., P06) or outside the Punta
730 Leysser DSGSD area (i.e., SNA 16/02 and SNA16/03), show a good degree of
731 development and are identifiable as *Sols Brunifiés* (Duchaufour, 1995).
732 In fact, in both study sites, the soil profiles located along the slopes (i.e., P01, P02,
733 P03, P07, SN01, and SN05) and at the gully edge (i.e., SNA16/01, SN03, and
734 partially P04) are characterised by a weak degree of development, probably caused by
735 the continuous sedimentation/erosion phases deriving from colluvial events and
736 water-driven erosion.
737 Anyway, the two study sites also show some dissimilarity from a geopedological
738 point of view. The alternation of aggradation/degradation episodes along the slopes
739 are testified only in the SN study site by a buried surface underlined by the presence
740 of grain size discontinuity and by a peak of organic carbon content (i.e., SN03-2AC
741 and SN01-2A horizons); whereas, no buried surfaces are found in the GG study site.
742 Nevertheless, a little grain-size discontinuity is found in P07, probably caused by the

743 incorporation along the profile of coarse material transported by water-driven
744 processes or snow action.
745 Hence, dendrogeomorphological indicators (different response in the two sites) and
746 geopedological techniques (different degree of soil development and
747 presence/absence of buried surface) agree in detecting differences in surface
748 geomorphic processes inducing erosion along slopes in the sites: higher in GG and
749 lower in SN. The application of LERs and AERs allowed both for delineating the
750 local and general trend of erosion.
751 A discussion may be open on the role of geostructural drivers in triggering erosion,
752 combining, hence, the geomorphological and structural conditions characterising the
753 study sites (Fort, 2000; Cossart et al., 2013). The structural conditions may in fact
754 guide, at first, the localisation of the relatively deep incisions along the slopes, prepare
755 a weaker substrate on which erosional processes could easily act, or, again, trigger the
756 erosion rates in relation with Earth surface uplift or lowering. For example, according
757 to different authors (Pini et al., 2013; Forno et al., 2016), the Punta Leysser DSGSD
758 dynamics guided the Quaternary history of the slope in the SN case, in particular, the
759 preservation of Quaternary sediments. Considering, moreover, the asymmetric shape
760 of the SN site (more linear on the western sites and articulated in subbasins along the
761 eastern side), this nonlinearity in erosion patterns may be related to the location of the
762 gully up above the westward diversion of the western edge of the Punta Leysser
763 DSGSD, probably inducing water flow variations. Because, moreover, gully systems
764 are usually characterised by step-like erosional trends, as detected in Mediterranean
765 contexts by Della Seta et al. (2009), these trends may be exasperated by the
766 differential movements especially along the border zones of DSGSDs (Mortara and
767 Sorzana, 1987). As indicated before, the AER along the western scarp of the SN site

768 (B1 along the DSGSD edge) is 1.32 cm/y that is slightly higher if compared with the
769 AER on similar deposits in Alpine areas indicated before (i.e., 0.58 cm/y). Also in the
770 GG case, the AER along the scarp edge is higher (2.81 cm/y), with local significant
771 peaks (i.e., 30.57 cm/y). However, if at the SN case the Punta Leysser DSGSD
772 pervasively characterises the slope, there are no signs of a DSGSD surveyed in the
773 GG site by previous authors (Cadoppi et al., 2007). Instead, in the GG case, the slope
774 is very steep and geomorphic processes, related for example to snow action (Sacco,
775 1921; Cadoppi et al., 2002) or gravity (i.e., debris falls), may have contributed
776 significantly to denudation, as demonstrated in other morphoclimatic contexts (Bollati
777 et al., 2016a).
778 These findings are also confirmed by the soil profiles along the GG slope, which are
779 continuously reworked and do not present any buried surface. Moreover, the deep
780 incision, as described before, may be considered a further triggering of scarp
781 instability, linked with the improbable further regressive evolution of the gully,
782 impeded by the presence of the upstream valley shaped in the bedrock (i.e., marble
783 bank of the DM unit herein in structural contact with the SU unit).
784 The results summarised in Table 3 and herein discussed allow us for tracing some
785 final considerations regarding the sites and the related dynamics: (i) AERs are
786 comparable and higher than in other contexts; (ii) denudation processes (e.g., mass
787 wasting, snow avalanches) favoured by a more exposed and steeper slope and testified
788 by the presence of specific indicators, revealed by trees and soils analyses, could be
789 considered more influent in the GG site area, and (iii) since the erosional intensity is
790 similar at the SN site but, at the same time, geomorphic processes responsible for
791 denudation seem currently less active at SN than in the GG area, structural conditions

related to DSGSD presence could be invoked as responsible for the similar erosion rates.

According to these interpretations, the acquired results contribute to delineation in more detail of the scientific value of the sites and the strengthening of the importance of considering slope evolution in the framework of geoheritage evaluation (e.g., Bollati et al., 2018). This consideration has fallouts in term of dissemination and educational applications (e.g., Pelfini et al., 2016). In the case of SN, the link with the presence of the Punta Leysser DSGSD is not mentioned in the documentation available for *geosite SN*, but it should be considered relevant for explaining the complexity of interaction between different factors in SN slope evolution. Concerning *geosite GG*, the site was hypothesised to be formed during a single extreme event (Regione Piemonte, 1995) even though no data was provided supporting this hypothesis. No data coming from this investigation supports or contrasts this hypothesis, on the contrary there was evidence of the relevance of a constant action by surface geomorphic processes interacting with the GG evolution. Hence, in the framework of dissemination of physical landscape evolution, it seems appropriate to consider the analysed geosites in the contexts of the respective slope evolution (i.e., geological, structural, geomorphological drivers). Moreover, their relation with climate trends and vegetation dynamics as ecological indicators of geomorphic activity is relevant (e.g., Bollati et al., 2015; Pelfini et al., 2016; Bollati et al., 2018) as their development cannot be disconnected from their own slope history.

6. Conclusions

The study sites of Gran Gorgia (GG) and Saint Nicolas (SN) are two gully complex systems developed in glacial deposits on which water-driven processes in relation to local factors (i.e., geological, geomorphological, structural, and climate features) are producing relevant landscapes (i.e., pseudo-badlands feature). Multidisciplinary analyses performed at these sites allowed us for acquiring details on erosional history of the studied slopes. Common and dissimilar traits were detected using trees and soils, and local and average erosion rates were calculated and compared with other morphogenetic and morphoclimatic contexts. The results were discussed and a prevalence of geomorphological constraints on evolution was detected at the GG site, while at the SN site a probable stronger influence of the structural background was considered. The novelty of this work is represented by the multidisciplinary approach used to detect the relationship existing between denudation processes, geological structures, soils and vegetation and their precious roles for analysing applied geomorphology issues. Because the sites have already been classified as geosites by local authorities, their scientific relevance could benefit from the data obtained in the prese,nt research on their genesis, evolution, and local drivers affecting the rates of denudation, connected with the entire slope history. New data, herein presented, represents, moreover, a starting point for Geosciences education.

Acknowledgements

The authors are sincerely grateful to the two anonymous reviewers and to the editors who significantly improved the manuscript. The research was carried out in the framework of the following projects: (i) PRIN 2010–2011 project (grant number 2010AYKTAB_006) ‘Response of morphoclimatic system dynamics to global changes and related geomorphological hazards’; (ii) Fondi Potenziamento della

Ricerca - Linea 2 – 2015 Project ‘Dynamic of active margins: from rift to collisional chains’, leader Dr. Davide Zanoni. The authors thank: (i) Prof. G. Forno and Prof. M. Gattiglio for the fruitful discussions on the site of Saint Nicolas; (ii) G. Volpi, Dr. E. Miascotti, and Dr. M. Pellegrini for the collaboration in the field and during the elaboration of the geopedological and dendrogeomorphological analysis in the laboratory; (iii) Daniele Cat Berro (SMI, Italian Society of Meteorology), Arpa Piemonte, and Arpa Valle d’Aosta for validating and providing meteorological records; (iv) Antonio Borello, Ente di Gestione dei Parchi delle Alpi Cozie for helpful assistance in the field and the sharing of information. The authors are also grateful to the local public administration that provided the permits to sample vegetation, to collect soil samples, and to use the private roads.

References

Aigotti, D., Baggio, P., Bois, M.; Cadoppi, P., Costamagna, A. Deline, P., De Renzo, G., Ghelli, A; Giardino, M., Giordan, D., Mortara, G., Nervo, B., Pellegrino, P., Perotti, L., Riccio, I., Rossato, C., Rossi, C., 2004. I geositi nel paesaggio della Provincia di Torino, Litografia Geda per la Provincia di Torino, Turin, Italy. http://www.provincia.torino.gov.it/territorio/file-storage/download/pdf/dif_suolo/geositi/gran_gorgia.pdf.

Alestalo, J., 1971. Dendrochronological interpretation of geomorphic processes. Fennia 105, 140 pp.

Alexander, D.E., 1980. I calanchi-accelerated erosion in Italy. Geography 65(2), 95-100.

865 Anselmo, V., Di Nunzio, F., Godone, F., 1975. Torrente (Il) Prebec in territorio di
866 Chianocco (Valle di Susa). Studi ideologici e ricerche storiche. CNR - Laboratorio
867 di Ricerca per la Protezione Idrogeologica nel Bacino Padano, Rapporto interno
868 M.I. 75/1, Turin, 33 pp.
869 Ballantyne, C.K., 2002. A general model of paraglacial landscape response. Holocene
870 12(3), 371-376. https://doi.org/10.1191/0959683602hl553fa.
871 Bollati, I., Leonelli, G., Vezzola, L., Pelfini, M., 2015. The role of ecological value in
872 geomorphosite assessment for the debris-covered Miage Glacier (Western Italian
873 Alps) based on a review of 2.5 centuries of scientific study. Geoheritage 7(2), 119-
874 135. https://doi.org/10.1007/s12371-014-0111-2.
875 Bollati, I., Vergari, F., Del Monte, M., Pelfini, M., 2016a. Multitemporal
876 dendrogeomorphological analysis of slope instability in Upper Orcia Valley
877 (Southern Tuscany, Italy). Geogr. Fis. Din. Quat. 39(2), 105-120.
878 https://doi.org/10.4461/ GFDQ 2016.39.10.
879 Bollati, I., Reynard, E., Palmieri, E.L., Pelfini, M., 2016b. Runoff impact on active
880 geomorphosites in unconsolidated substrate. A comparison between landforms in
881 glacial and marine clay sediments: two case studies from the Swiss Alps and the
882 Italian Apennines. Geoheritage 8(1), 61-75. https://doi.org/10.1007/s12371-015-
883 0161-0.
884 Bollati, I., Pellegrini, M., Reynard, E., Pelfini, M., 2017. Water driven processes and
885 landforms evolution rates in mountain geomorphosites: examples from Swiss Alps.
886 Catena 158, 321-339. https://doi.org/10.1016/j.catena.2017.07.013.
887 Bollati, I, Crosa Lenz, B., Golzio, A., Masseroli, A., 2018. Tree rings as ecological
888 indicator of geomorphic activity in geoheritage studies. Ecol. Ind. 93, 899-916.
889 https://doi.org/10.1016/j.ecolind.2018.05.053.

Bollschweiler, M., Stoffel, M., Schneuwly, D.M., Bourqui, K., 2008. Traumatic resin ducts in Larix decidua stems impacted by debris flows. Tree Physiol. 28(2), 255-263. https://doi.org/10.1093/treephys/28.2.255.

Brilha, J., 2016. Inventory and quantitative assessment of geosites and geodiversity sites: a review. Geoheritage 8(2), 119-134. https://doi.org/10.1007/s12371-014-0139-3.

Burga, C.A., Krüsi, B., Egli, M., Wernli, M., Elsener, S., Ziefle, M., Fischer, T., Mavris, C., 2010. Plant succession and soil development on the foreland of the Morteratsch glacier (Pontresina, Switzerland): Straight forward or chaotic?. Flora-Morphology, Distribution, Funct. Ecol. Plants 205(9), 561-576. https://doi.org/10.1016/j.flora.2009.10.001.

Cadoppi, P., Castelletto, M., Sacchi, R., Baggio, P., Carraro, F., Giraud, V., 2002. Carta Geologica d'Italia alla scala 1:50.000 - Foglio 154, Susa. 1 map, scale 1:50000, ISPRA, Rome.

Cadoppi, P., Giardino, M., Perrone, G., Tallone, S., 2007. Litho-structural control, morphotectonics, and deep-seated gravitational deformations in the evolution of Alpine relief: a case study in the lower Susa Valley (Italian Western Alps). Quat. Int. 171, 143-159. https://doi.org/10.1016/j.quaint.2006.10.015.

Chiarle M., Mortara G., 2001. Esempi di rimodellamento di apparati morenici nell'arco alpino italiano. Suppl. Geogr. Fis. Dinam. Quat. V, 41-54.

Chiarle, M., Iannotti, S., Mortara, G., Deline, P., 2007. Recent debris flow occurrences associated with glaciers in the Alps. Global Planet. Change 56(1-2), 123-136. https://doi.org/10.1016/j.gloplacha.2006.07.003.

913 Compostella, C., Trombino, L., Caccianiga, M., 2013. Late Holocene soil evolution
914 and treeline fluctuations in the Northern Apennines. Quat. Int. 289, 46-59.
915 https://doi.org/10.1016/j.quaint.2012.02.011.
916 Cossart, E., Fort, M., 2008. Sediment release and storage in early deglaciated areas:
917 towards an application of the exhaustion model from the case of Massif des Écrins
918 (French Alps) since the Little Ice Age. Norw. J. Geogr. 2(2), 115-131.
919 https://doi.org/10.1080/00291950802095145.
920 Cossart, E., Mercier, D., Decaulne, A., Feuillet, T., 2013. An overview of the
921 consequences of paraglacial landsliding on deglaciated mountain slopes: typology,
922 timing and contribution to cascading fluxes. Quaternaire 24(1), 13-24.
923 https://doi.org/10.4000/quaternaire.6444.
924 Cruden, D.M., Hu, X.Q., 1993. Exhaustion and steady state models for predicting
925 landslide hazards in the Canadian Rocky Mountains. Geomorphology 8(4), 279-
926 285. https://doi.org/10.1016/0169-555X(93)90024-V.
927 Curry, A.M., 1999. Paraglacial modification of slope form. Earth Surf. Proc. Land.
928 24(13), 1213-1228. https://doi.org/10.1002/(SICI)1096-
929 9837(199912)24:13<1213::AID-ESP32>3.0.CO;2-B.
930 De Luca, D., Destefanis, E., Forno, M.G., Fratianni, S., Gattiglio, M., Masciocco, L.,
931 Menegon, A., 2009. Studio interdisciplinare per il monitoraggio e la valorizzazione
932 delle sorgenti della valle Susa in previsione di opere a forte impatto ambientale.
933 Memorie Della Società Geografica Italiana 87, 189-199.
934 Della Seta, M., Del Monte, M., Fredi, P., Palmieri, E. L., 2009. Space–time variability
935 of denudation rates at the catchment and hillslope scales on the Tyrrhenian side of
936 Central Italy. Geomorphology 107(3-4), 161-177.
937 https://doi.org/10.1016/j.geomorph.2008.12.004.

938 Duchaufour, P., 1995. Pedology. Soil, vegetation, environment. Ed. 4th, CRC Press,
939 Boca Raton, USA, 274 pp.
940 Eichel, J., Corenblit, D., Dikau, R., 2016. Conditions for feedbacks between
941 geomorphic and vegetation dynamics on lateral moraine slopes: a biogeomorphic
942 feedback window. Earth Surf. Proc. Land. 41(3), 406-419.
943 https://doi.org/10.1002/esp.3859.
944 Farifteh, J., Soeters, R., 2006. Origin of biancane and calanchi in East Aliano,
945 southern Italy. Geomorphology 77(1-2), 142-152.
946 https://doi.org/10.1016/j.geomorph.2005.12.012.
947 Forno, M.G., Gattiglio, M, Gianotti, F., 2012. Geological context of the Becca France
948 historical landslide (Aosta Valley, NW Italy). Alpine and Mediterranean
949 Quaternary 25(2), 125-140.
950 Forno, M.G., Gattiglio, M., Gianotti, F., Guerreschi, A., Raiteri, L., 2013. Deep-
951 seated gravitational slope deformations as possible suitable locations for
952 prehistoric human settlements: an example from the Italian Western Alps. Quat.
953 Int., 303, 180-190. https://doi.org/10.1016/j.quaint.2013.03.033.
954 Forno, M.G., Comina, C., Gattiglio, M., Gianotti, F., Lo Russo, S., Raiteri, L.,
955 Sambuelli L., Taddia, G., 2016. Preservation of Quaternary sediments in DSGSD
956 environments: the Mont Fallère case study (Aosta Valley, NW Italy). Alpine and
957 Mediterranean Quaternary 29(2), 181-191.
958 Fort, M., 2000. Glaciers and mass wasting processes: their influence on the shaping of
959 the Kali Gandaki valley (higher Himalaya of Nepal). Quat. Int. 65, 101-119.
960 https://doi.org/10.1016/S1040-6182(99)00039-7.

961 Frei, C., Schär, C., Lüthi, D., Davies, H.C., 1998. Heavy precipitation processes in a
962 warmer climate. Geophys. Res. Lett. 25(9), 1431-1434.
963 https://doi.org/10.1029/98GL51099.
964 Galeandro, A., Doglioni, A., Guerricchio, A., Simeone, V., 2013. Hydraulic stream
965 network conditioning by a tectonically induced, giant, deep-seated landslide along
966 the front of the Apennine chain (south Italy). Nat. Hazards Earth Sys. 13(5), 1269-
967 1283. https://doi.org/10.5194/nhess-13-1269-2013.
968 Garavaglia, V., Pelfini, M., 2011. The role of border areas for dendrochronological
969 investigations on catastrophic snow avalanches: a case study from the Italian Alps.
970 Catena 87(2), 209-215. https://doi.org/10.1016/j.catena.2011.06.006.
971 Gärtner H., 2007. Tree roots - methodological review and new development in dating
972 and quantifying erosive processes. Geomorphology 86, 243–251.
973 https://doi.org/10.1016/j.geomorph.2006.09.001.
974 Gianotti, F., Forno, M.G., Ivy-Ochs, S., Monegato, G., Pini, R., Ravazzi, C., 2015.
975 Stratigraphy of the Ivrea Morainic Amphitheatre (NW Italy). An updated
976 synthesis. Alpine and Mediterranean Quaternary 28(1), 29-58.
977 Giardino, M., Mortara, G., Chiarle, M., 2017. The glaciers of the Valle d'Aosta and
978 Piemonte regions: records of present and past environmental and climate changes.
979 In: Soldati, M., Marchetti, M. (Eds.), Landscapes and Landforms of Italy, Springer,
980 Cambridge, pp. 77-88.
981 Giordano, E., Giardino, M., Perotti, L., Ghiraldi, L., Palomba, M., 2016. Following
982 the tracks of Charlemagne in the Cottian Alps. The cultural and geological heritage
983 of the Franks Trail (Susa Valley, Piemonte, NW Italy). Geoheritage 8(4), 293-300.
984 https://doi.org/10.1007/s12371-015-0158-8.

985 Guida, D., Pelfini, M., Santilli, M., 2008. Geomorphological and dendrochronological
986 analyses of a complex landslide in the Southern Apennines. Geogr. Ann.: Ser. A,
987 Phys. Geogr. 90(3), 211-226. https://doi.org/10.1111/j.1468-0459.2008.340.x.
988 Hinderer, M., 2001. Late Quaternary denudation of the Alps, valley and lake fillings
989 and modern river loads. Geodin. Acta 14(4), 231-263.
990 https://doi.org/10.1080/09853111.2001.11432446.
991 Holmes, R.L., Adams, R.K., Fritts, H.C., 1986. Tree-ring chronologies of North
992 America: California, Eastern Oregon and Northern Great Basin with procedures
993 used in the chronology development work including user manual for computer
994 program COFECHA and ARSTAN. Chronology Series VI. University of Arizona,
995 Laboratory of Tree-Ring Research, Tucson, USA.
996 Hupp, C.R., Carey, W.P., 1990. Dendrogeomorphic approach to estimating slope
997 retreat, Maxey Flats, Kentucky. Geology 18(7), 658-661.
998 IPLA, 2007. Carta dei suoli del Piemonte, 1 map, 1:250000. S.EL.CA. Ed.
999 Ivy- Ochs, S., Lucchesi, S., Baggio, P., Fioraso, G., Gianotti, F., Monegato, G., Graf,
1000 A., Akçar N., Christl, M., Carraro, F., Forno, M.G., Schlüchter, C., 2018. New
1001 geomorphological and chronological constraints for glacial deposits in the
1002 Rivoli- Avigliana end- moraine system and the lower Susa Valley (Western Alps,
1003 NW Italy). J. Quat. Sci. 33(5), 550-562. https://doi.org/10.1002/jqs.3034.
1004 Keiler, M., Knight, J., Harrison, S., 2010. Climate change and geomorphological
1005 hazards in the Eastern European Alps. Philos. T. Roy. Soc. A. 368(1919), 2461-
1006 2479. https://doi.org/10.1098/rsta.2010.0047.
1007 Kogelnig-Mayer, B., Stoffel, M., Schneuwly-Bollschweiler, M., Hübl, J., Rudolf-
1008 Miklau, F., 2011. Possibilities and limitations of dendrogeomorphic time-series
1009 reconstructions on sites influenced by debris flows and frequent snow avalanche

activity. Arct. Antarct. Alp. Res. 43(4), 649-658. https://doi.org/10.1657/1938-4246-43.4.649.

Korup, O., 2005. Geomorphic imprint of landslides on alpine river systems, southwest New Zealand. Earth Surf. Proc. Land. 30(7), 783-800. https://doi.org/10.1002/esp.1171.

Lucchesi, S., Gianotti, F., Giardino, M., 2015. The Morainic Amphitheatre Environment: a geosite to rediscover the geological and cultural heritage in the examples of the Ivrea and Rivoli-Avigliana Morainic Amphitheatres (NW Italy). In: Lollino G. et al. (Eds.): Engineering geology for society and territory - Volume 8: Preservation of Cultural Heritage, Springer, Cham, pp. 213-216. https://doi.org/10.1007/978-3-319-09408-3_41.

McColl, S.T., 2012. Paraglacial rock-slope stability. Geomorphology 153, 1-16, https://doi.org/10.1016/j.geomorph.2012.02.015.

Mercalli, L., Cat Berro, D., Montuschi, S., 2003. Atlante climatico della valle d'Aosta. Turin, Società Meteorologica Subalpina, 416 pp.

Mercier, D., Étienne, S., Sellier, D., André, M.F., 2009. Paraglacial gullying of sediment - mantled slopes: a case study of Colletthøgda, Kongsfjorden area, West Spitsbergen (Svalbard). Earth Surf. Proc. Land. 34(13), 1772-1789. https://doi.org/10.1002/esp.1862.

Ministero delle Risorse Agricole Alimentari e Forestali, 1994. Metodi ufficiali di analisi chimica del suolo, con commenti ed interpretazioni. ISMEA, Roma, 207 pp.

Mortara, G., 1975. Osservazioni preliminari nel bacino del Torrente Prebec (Valle di Susa). CNR-IRPI Torino Ed., 36 pp.

1033 Mortara, G., Sorzana, P., 1987. Fenomeni di deformazione gravitativa profonda
1034 nell'arco alpino occidentale italiano. Considerazioni litostrutturali e morfologiche,
1035 Boll. Soc. Geol. It. 42, 203-244.
1036 Mortara, G., Turitto, O., 1989. Considerazioni sulla vulnerabilità di alcuni siti adibiti
1037 a campeggio in ambiente alpino. In: Badino V. (Ed.), Suolosottosuolo -
1038 Proceedings of the International Congress on Geoengineering, Litografica Geda,
1039 Turin, 1, 137-144.
1040 Mortara, G., Dutto, F., Godone, F., 1995. Effetti degli eventi alluvionali nell'ambiente
1041 proglaciale. La sovraincisione della morena del Ghiacciaio del Mulinet (Stura di
1042 Valgrande, Alpi Graie). Geogr. Fis. Din. Quat. 18, 295-304.
1043 Panizza, M., 2001. Geomorphosites: concepts, methods and examples of
1044 geomorphological survey. Chinese Sci. Bull. 46(1), 4-5.
1045 https://doi.org/10.1007/BF03187227.
1046 Pelfini, M., Bollati, I., 2014. Landforms and geomorphosites ongoing changes:
1047 concepts and implications for geoheritage promotion. Quaestiones geographicae
1048 33(1), 131-143. https://doi.org/10.2478/quageo-2014-0009.
1049 Pelfini, M., Santilli, M., 2008. Frequency of debris flows and their relation with
1050 precipitation: a case study in the Central Alps, Italy. Geomorphology 101(4), 721-
1051 730. https://doi.org/10.1016/j.geomorph.2008.04.002.
1052 Pelfini, M., Leonelli, G., Trombino, L., Zerboni, A., Bollati, I., Merlini, A., Smiraglia,
1053 C., Diolaiuti, G., 2014. New data on glacier fluctuations during the climatic
1054 transition at~ 4,000 cal. year BP from a buried log in the Forni Glacier forefield
1055 (Italian Alps). Rend. Lin. 25(4), 427-437. doi.org/10.1007/s12210-014-0346-5

1056 Pelfini, M., Bollati, I., Pellegrini, L., Zucali, M., 2016. Earth Sciences on the field:
1057 educational applications for the comprehension of landscape evolution. Rend.
1058 Online Soc. Geol. It., 40, 56-66. https://doi.org/10.3301/ROL.2018.19.
1059 Pini, R., Guerreschi, A., Raiteri, L., Ravazzi, C., 2013. Preistoria degli ambienti d'alta
1060 quota in Valle d'Aosta. Primi risultati di indagini paleobotaniche e archeologiche
1061 sull'altopiano del Monte Fallère. Bull. Et. Preh. Archéol. Alp. 23, 2012-2013.
1062 Polino, R., Bonetto, F.; Carraro, F., Gianotti, F., Gouffon, Y., Malusà, M.G., Martin,
1063 S., Perello, P., Schiavo, A., 2015. Carta Geologica d'Italia. Foglio 90 - Aosta. 1
1064 map, scale 1:50000, ISPRA, Rome.
1065 Régent Instrument Inc., 2001. WinDENDRO 2001. Quebec, Canada
1066 Regione Piemonte, 1995. Atlante Toponomastico del Piemonte Montano - Chianocco,
1067 5. Sottocategoria Toponomastica. Dell'Orso Ed., Torino, 144 pp.
1068 Reynard, E., Fontana, G., Kozlik, L., Scapozza, C., 2007. A method for assessing
1069 "scientific" and "additional values" of geomorphosites. Geogr. Helv. 62(3), 148-
1070 158. https://doi.org/10.5194/gh-62-148-2007.
1071 Rinn, F., 1996. TSAP. Time Series Analysis and Presentation. Version 3.0 Reference
1072 Manual, Heidelberg.
1073 Sacco, F., 1921. Il glacialismo della Valle di Susa. L'universo, 2, 561-592.
1074 Sacco, F., 1927. Il glacialismo nella Valle D'Aosta: memoria del prof. Federico
1075 Sacco. Provveditorato generale dello Stato. Ed. Checchini, Torino, 66 pp.
1076 Smiraglia, C., Azzoni, R.S., D'Agata, C., Maragno, D., Fugazza, D., Diolaiuti, G.A.,
1077 2015. The evolution of the Italian glaciers from the previous data base to the New
1078 Italian Inventory. Preliminary considerations and results. Geogr. Fis. Din. Quat.
1079 38(1), 79-87. https://doi.org/10.4461/GFDQ.2015.38.08.

1080 Stoffel, M., Bollschweiler, M., 2008. Tree – ring analysis in natural hazards research
1081 – an overview. Nat. Hazards Earth Syst. 8, 187–202. https://doi.org/10.5194/nhess-
1082 8-187-2008.
1083 Stoffel, M., Corona, C., Ballesteros-Cánovas, J. A., Bodoque J.M., 2013. Dating and
1084 quantification of erosion processes based on exposed roots. Earth Sci. Rev. 123,
1085 18-34. https://doi.org/10.1016/j.earscirev.2013.04.002.
1086 Timell T. E., 1986. Compression wood in gymnosperms. Springer-Verlag, Berlin, 221
1087 pp.
1088 Tropeano, D., Govi, M., Mortara, G., Turitto, O., Sorzana, P., Negrini, G., Arattano,
1089 M., 1999. Eventi alluvionali e frane nell'Italia Settentrionale (1975 - 1981). IRPI-
1090 CNR Ed., Torino, 280 pp. http://www.irpi.to.cnr.it/documenti/eventi7581.pdf.
1091 Tropeano, D., Luino, F., Turconi, L., 2006. Eventi di piena e frana in Italia
1092 settentrionale nel periodo 2002-2004. IRPI-CNR Ed., Torino, 171 pp.
1093 http://www.irpi.to.cnr.it/documenti/volume20022004.pdf.
1094 Wimbledon, W.A., 1999. GEOSITES - an International Union of Geological Sciences
1095 initiative to conserve our geological heritage. Polish Geological Institute Special
1096 Papers 2, 5- 8.
1097 Zgłobicki, W., Poesen, J., Cohen, M., Del Monte, M., García-Ruiz, J.M., Ionita, I.,
1098 Niacsu, L., Machová, Z., Martín-Duque, J.F., Nadal-Romero, E, Pica, A., Rey, F.,
1099 Solé-Benet, A., Stankoviansky, M., Stolz, C., 2017. The potential of permanent
1100 gullies in Europe as geomorphosites. Geoheritage 1-23. https://doi.
1101 10.1007/s12371-017-0252-1.

Tables captions list

Table 1

Sampling clusters and subclusters at Gran Gorgia and Saint Nicolas; the geomorphic context is described and the soils profiles and trees codes are indicated, as used in the text

Table 2

Morphometric analyses at the study sites: (A) Morphometric measurements of the gullies (AR: altitudinal range, L: bottom length, W: average width, St: steepness; ΔA: altitude difference between edges); (B) Morphometric variations of surfaces affected by water runoff

Table 3

Prevailing disturbance indicators at the study areas

Table 1

Sampling clusters and subclusters at Gran Gorgia and Saint Nicolas; the geomorphic context is described and the soils profiles and trees codes are indicated, as used in the text

Geomorphic context	**GG**			**SN** *SN: along the Gaboè stream (B1)* *Rumiod: along the Montovret stream (B2)*		
	Soils	*Trees*	*Notes*	*Soils*	*Trees*	*Notes*
Slope	P01 P02 P03	A1	steep slope	SN 01 SN 05	B1.1	steep slope
	P07 P08	A2	counterscarp	/	/	/
Gully edge and peripheral streams	/	A3	upper W scarp	SN 03	B1.2	incipient gully (800 m N);
	P04	A4	lower W scarp	SNA 16/01 /	B1.3 B2	upper E scarp E scarp
Inside the gully	/	A5	along parallel transects	/	B1.4	inside the gully
Undisturbed (*reference conditions for soils and trees*)	P06	A6	within the forest (1.5 km SE; 1300 m a.s.l.);	SNA 16/02 SNA 16/03	/	outside the DSGD
	/	A7	within the forest (1 km SE; 1400 m a.s.l.).	/	B1.5	within the forest (1.3 km W, 1920 m a.s.l.)

Table 2

Morphometric analyses at the study sites: (A) Morphometric measurements of the gullies (AR: altitudinal range, L: bottom length, W: average width, St: steepness; ΔA: altitude difference between edges); (B) Morphometric variations of surfaces affected by water runoff

(A) Morphometric measurements

			AR (m asl)	L (m)	W (m)	S (%)	ΔA (m)
GG		max	1840	530	130	48.11	42
		min	1585				
		range	255				
SN		max	2000	1220	180	28.69	/
		min	1650				
		range	350				
SN Subtraits	*SN_i*	max	2000	430	170	18.60	10
		min	1920				
		range	80				
	SN_ii	max	1920	505	276	31.68	60
		min	1760				
		range	160				
	SN_iii	max	1760	285	93	38.60	< 10
		min	1650				
		range	110				

(B) Water runoff affected surface

		2012	**2007**	**1998**	**1997**	**1989**
GG	**Area (m^2)**	69679.14	69261.37	72293.47	72870.29	73492.48
	Variation (m^2)	417.77	-3032.10	-576.82	-622.19	
	% respect to previous measure	0.60	-4.19	-0.79	-0.85	
	Annual average	*83.55*	*-336.90*	*-576.82*	*-77.77*	
	% respect to previous measure	*0.12*	*-0.47*	*-0.79*	*-0.11*	
	Total widening: 2012-2007	**417.77**				
	Annual average	*83.55*				
	% respect to the first measure	***0.57***				
	Total reduction: 2007-1989		**-4231.11**			
	Annual average		*-235.06*			
	% respect to the first measure		***-5.76***			

		2012	**2006**	**1999**	**1997**	**1988**
SN	**Area (m^2)**	112967.32	121910.18	123197.94	127120.16	163454.70
	Variation (m^2)	-8942.86	-1287.76	-3922.22	-36334.54	
	% respect to previous measure	-7.34	-1.05	-3.09	-22.23	
	Annual average	*-1490.48*	*-183.97*	*-1961.11*	*-4037.17*	
	% respect to previous measure	*-1.22*	*-0.15*	*-1.54*	*-2.47*	
	Total reduction: 2012-1988			**-50487.38**		
	Annual average			*-2103.64*		
	% respect to the first measure			***-30.89***		

Table 3

Prevailing disturbance indicators at the study areas

	Relief evolution with related indicators at the study areas	
	Indicators	***Relevant examples***
GRAN GORGIA	*CW*	A3, A4, A5
	TRDs	A3, A4, A5
	Relevant erosion rates	A3, A4
	Weakly developed soils	P01, P02, P03
	Reworked soils with no buried surfaces	P07
SAINT NICOLAS	*Relevant erosion rates different along the DSDG edge and DSDG body*	B1.3, B2
	Oriented hydrographic pattern	B1.2; B1.3, B2
	Weakly developed soils	SN05, SNA16/01
	Alternation of aggradation/degradation episodes (i.e., buried surface)	SN01, SN03

Figures captions list

Fig. 1. Examples of the categories of gully developing on glacial deposits in the mountain environment. (A) Breach in the moraines primarily related to LIA and, secondarily, to the1920-1921 glacier advance at the Southern Mulinet Glacier in the Stura di Lanzo Valley (category 1 along the text); (B) Gran Gorgia deep gully cut in the upper Pleistocene glacial deposits along the northern flank of the lower Susa Valley (category 3 along the text); (C) Saint Nicolas calanchi, incised in glacial and fluvioglacial deposits on the northern side of the Aosta Valley (category 2 along the text). The satellite images used for each site are courtesy of ESRI, Digital Globe, GeoEye, earthstar Geographics, CNES Airbus DS, USDA, USGS, AeroGRID, IGN, and the GIS User Community.

Fig. 2. Iconography (upper and lower portion) and location of the study sites in northwestern Italy (in the middle). The locations of the Ivrea and the Rivoli-Avigliana morainic amphitheatres is reported as a reference of the Pleistocene maximum advance. The reaches of the Aosta and Susa valleys located between the study sites and the Pleistocene moraine amphitheatres are indicated in yellow. site A - Gran Gorgia: photo by G. Volpi, 2013; Site B1 - Saint Nicolas and B2 - Rumiod: photo by M. Pellegrini, 2016.

Fig. 3. Three examples of exposure year determination on roots from *Larix decidua* Mill. at GG site. In the low-right portion of the figure, a tilted stem inside the SN main gully is reported.

Fig. 4. Morphometric analysis on bare surface variations through time using orthophotos freely available through the Web Map Services (WMS) of the Geoportale Nazionale (http://www.pcn.minambiente.it/PCNDYN/catalogowms.jsp?lan=it). (A) Gran Gorgia; (B) Saint

Nicolas. In the middle, the graph of absolute surface variation (above) and of the percentages of average area variation related to their time interval (below).

Fig. 5. Local erosion rates (LERs) at the Gran Gorgia (A), Saint Nicolas (B1), and Rumiod (B2) samples clusters and subclusters. The indicated values are expressed in cm/y with the related year of exposure. The background images are three-dimensional prospects generated using Google Earth Pro 2017.

Fig. 6. Graphs showing the relation between TRDs (distinguishing between early, and latewood) and the number of trees (A) and between TRDs, CW and number of trees for the Gran Gorgia study site. In (B) the trees affected by TRDs and CW are expressed in percentage in respect to the trees germinated in that year. The 2014 and 2015 values are lower because of the lower number of trees added to the clusters during the second field campaign in 2016.

Fig. 7. Particle size distribution, organic C content, and pH values in the studied profiles of the Gran Gorgia study area. Particle size distribution plot: the gravel content is depicted in black, the sand content is depicted in dark grey the silt content is depicted in grey and the clay content is depicted in light grey. Only the gravel content data is available in horizons P01 OA, P02 O, P02 AC1, P02 AC2, P03 O, P06 O, and P08 AC2.

Fig. 8. Particle size distribution, organic C content, and pH values in the studied profiles of the Saint Nicolas study area. Particle size distribution plot: the gravel content is depicted in black, the sand content is depicted in dark grey, the silt content is depicted in grey, and the clay content is depicted in light grey.

Figure (Color)_1
Click here to download high resolution image

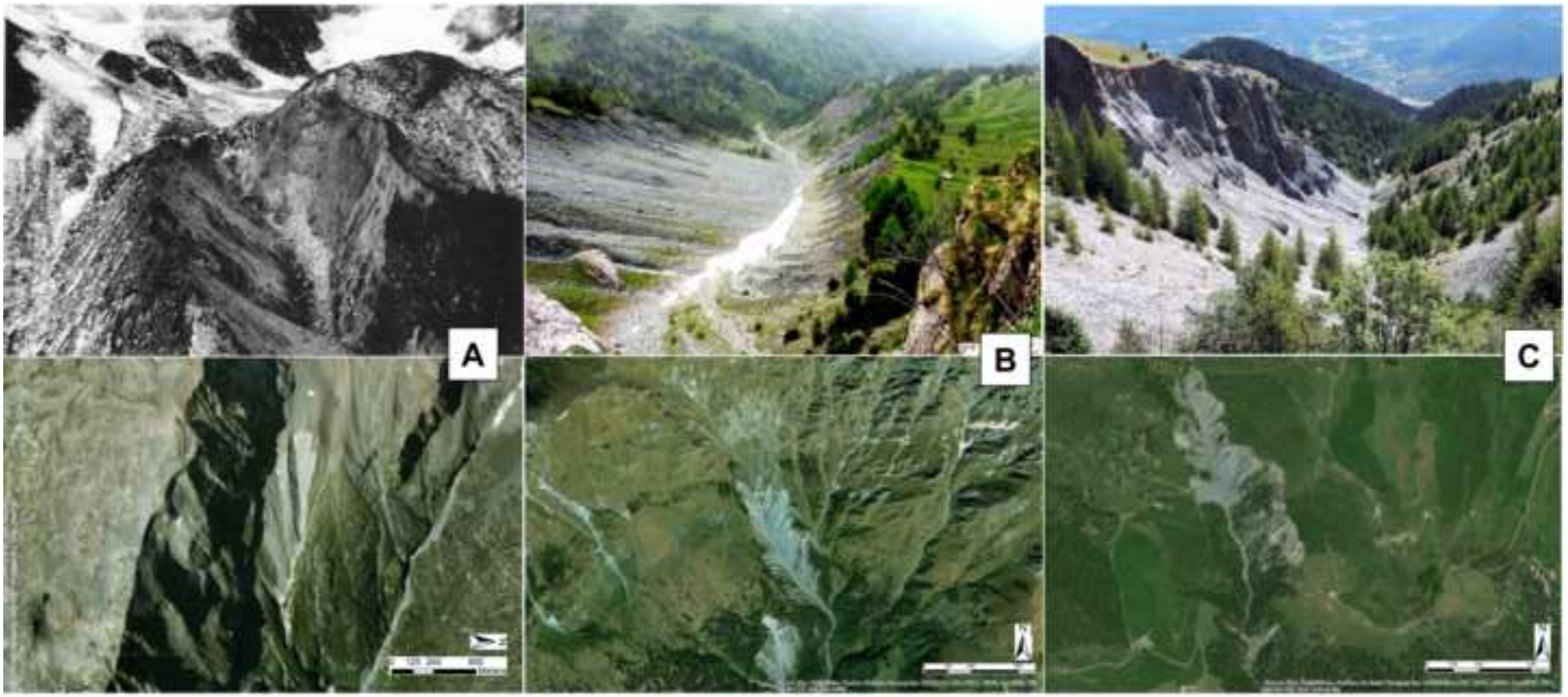

Figure (Color)_2

Click here to download high resolution image

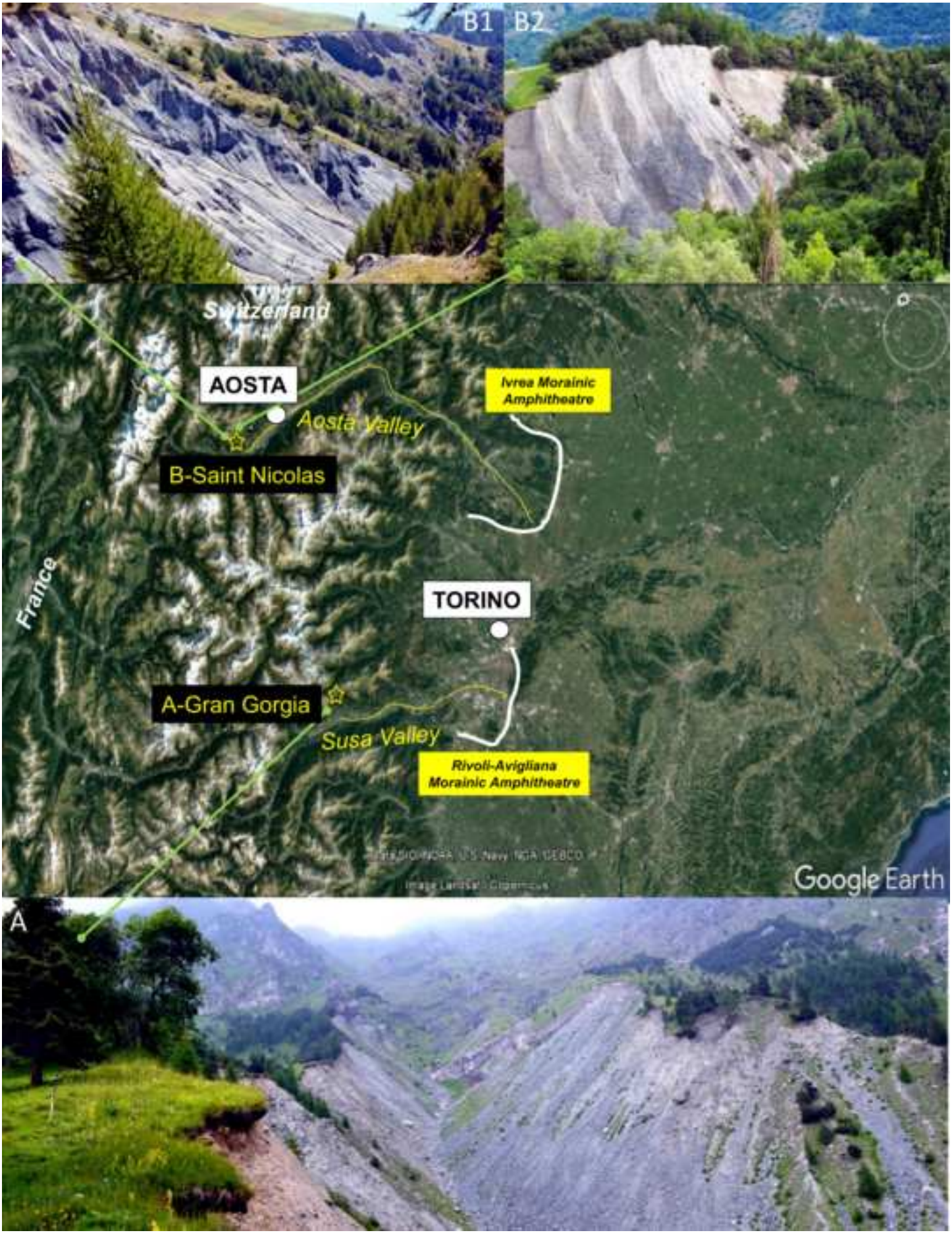

Figure (Color)_3_R2

Click here to download high resolution image

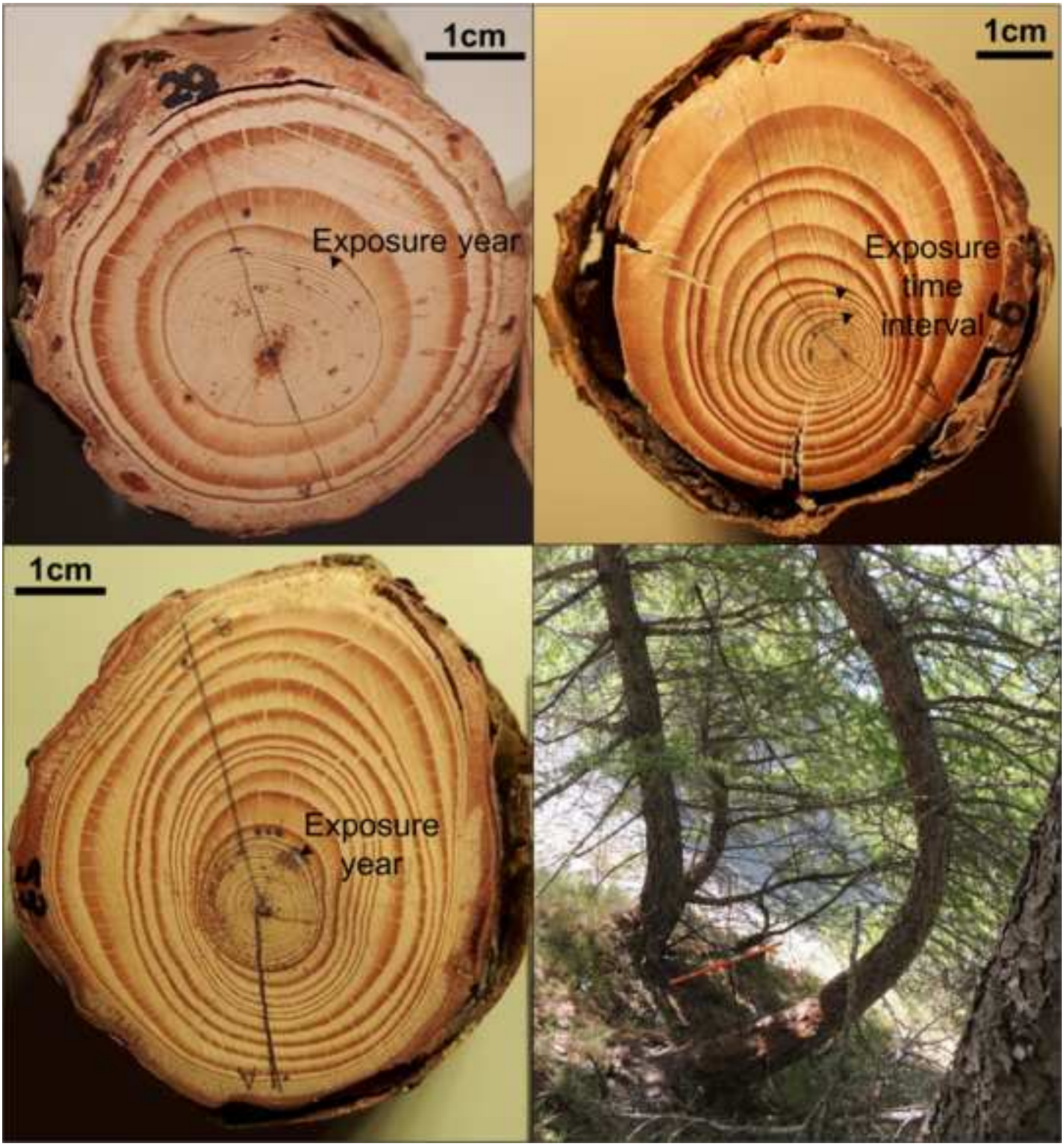

Figure (Color)_4_R1

Click here to download high resolution image

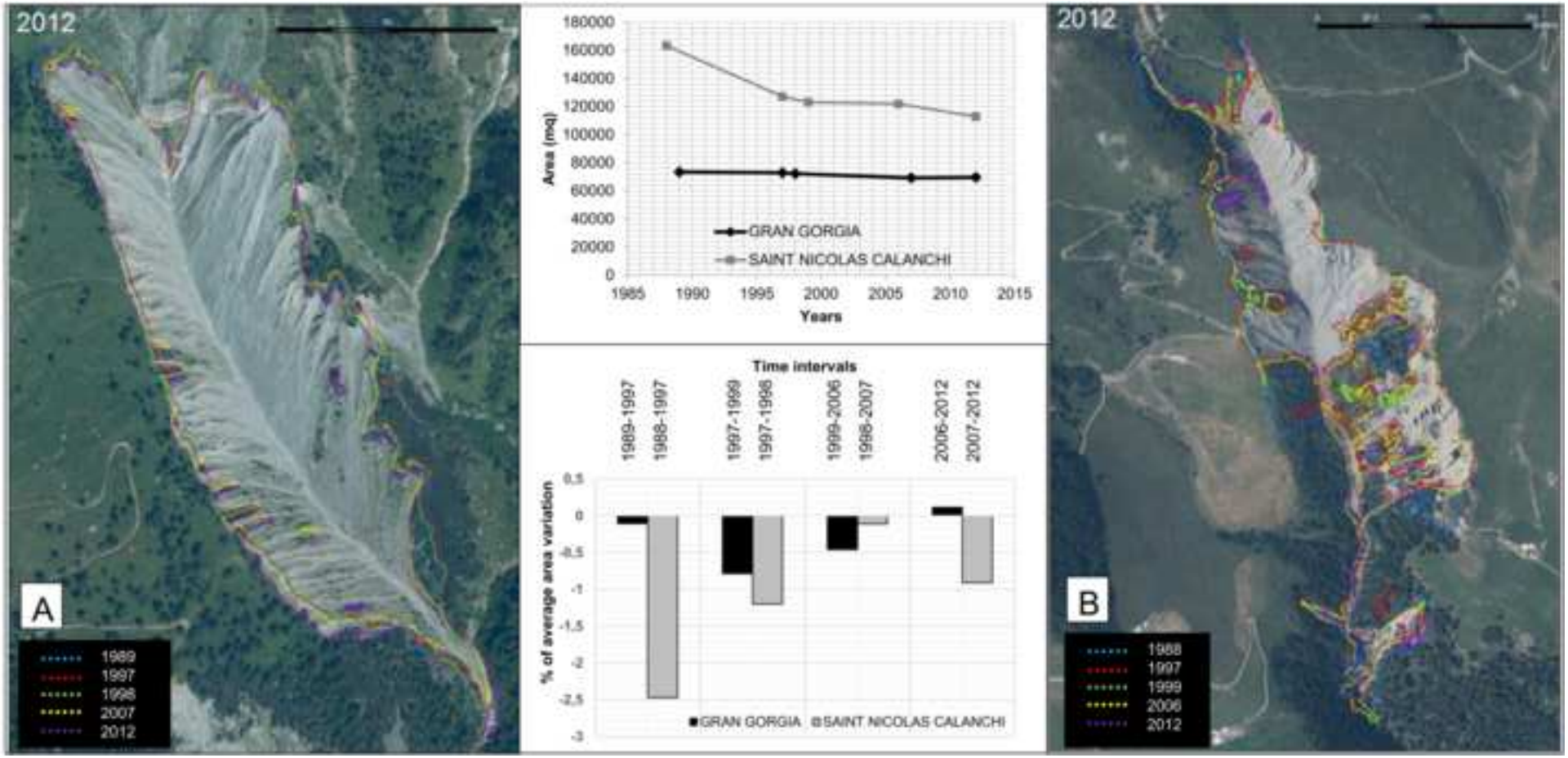

Figure (Color)_5_R1

Click here to download high resolution image

Figure (Greyscale)_1

Click here to download high resolution image

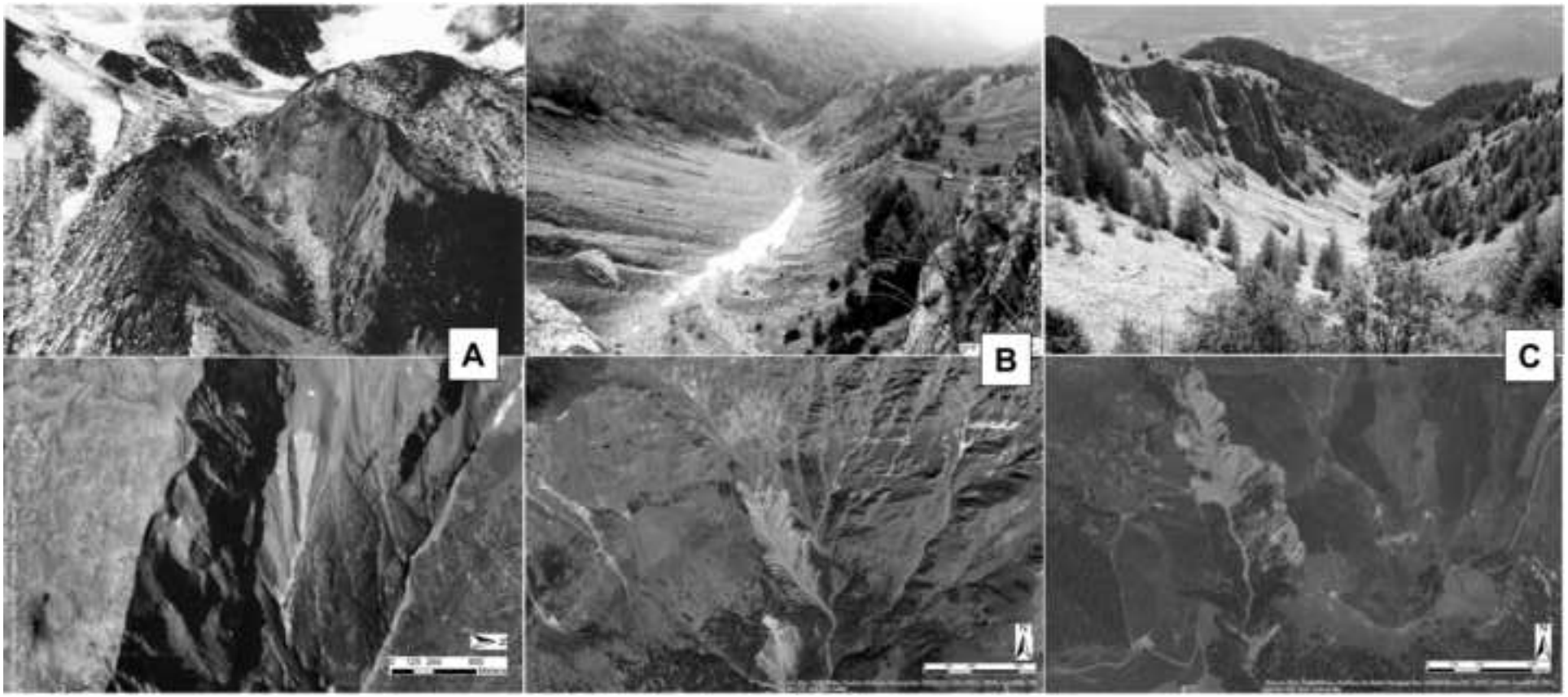

Figure (Greyscale)_2
Click here to download high resolution image

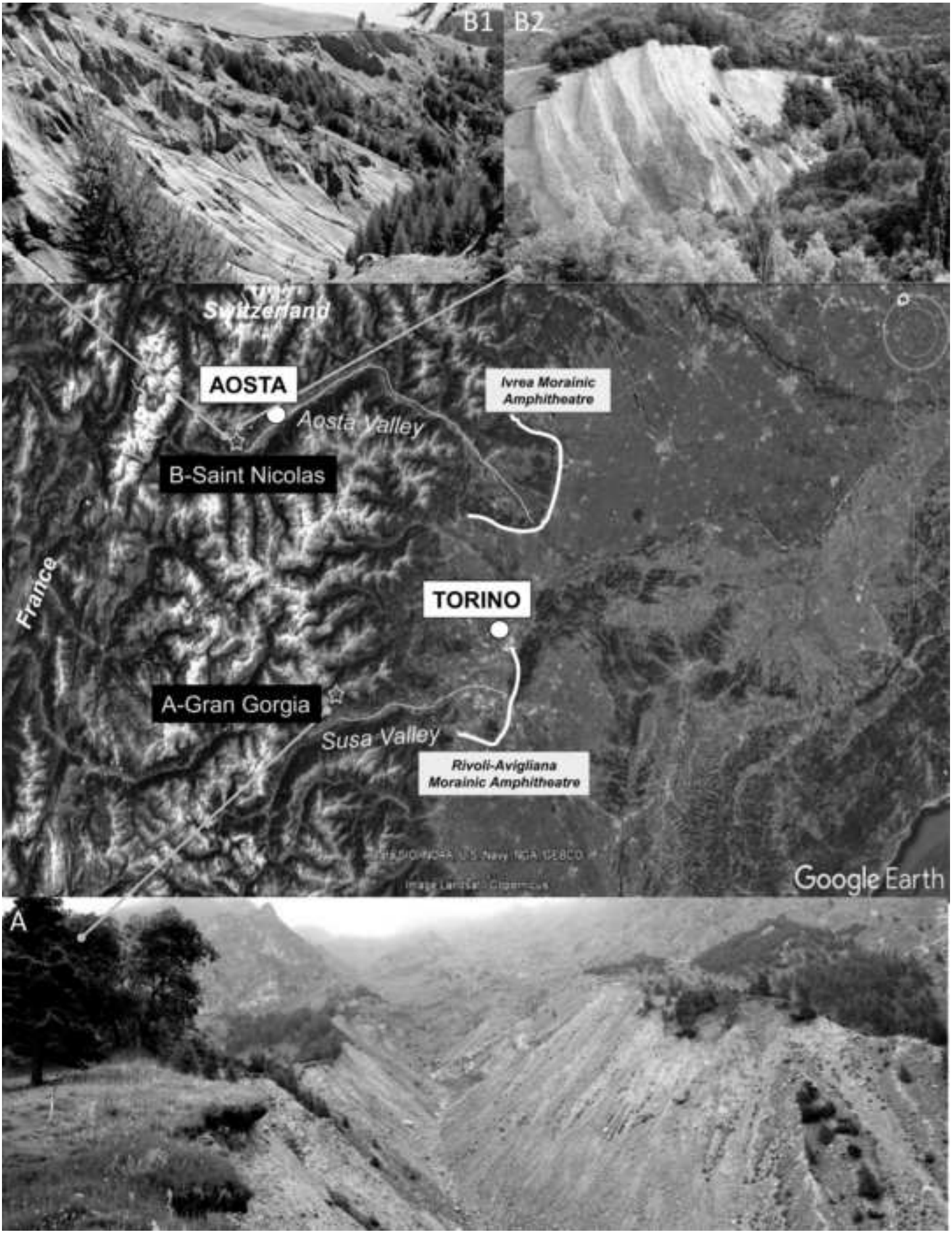

Figure (Greyscale)_3_R2
Click here to download high resolution image

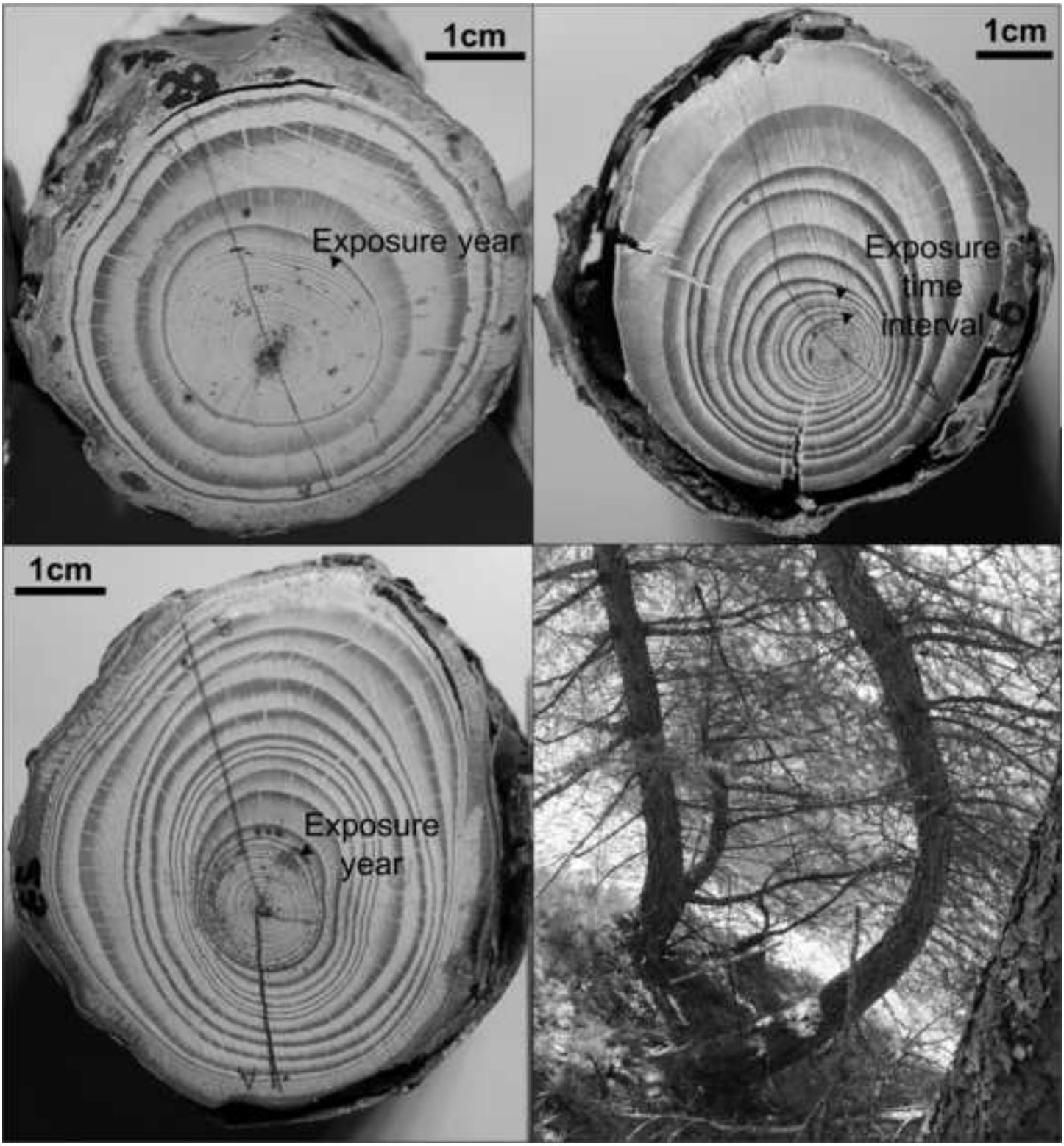

Figure (Greyscale)_4_R1

Click here to download high resolution image

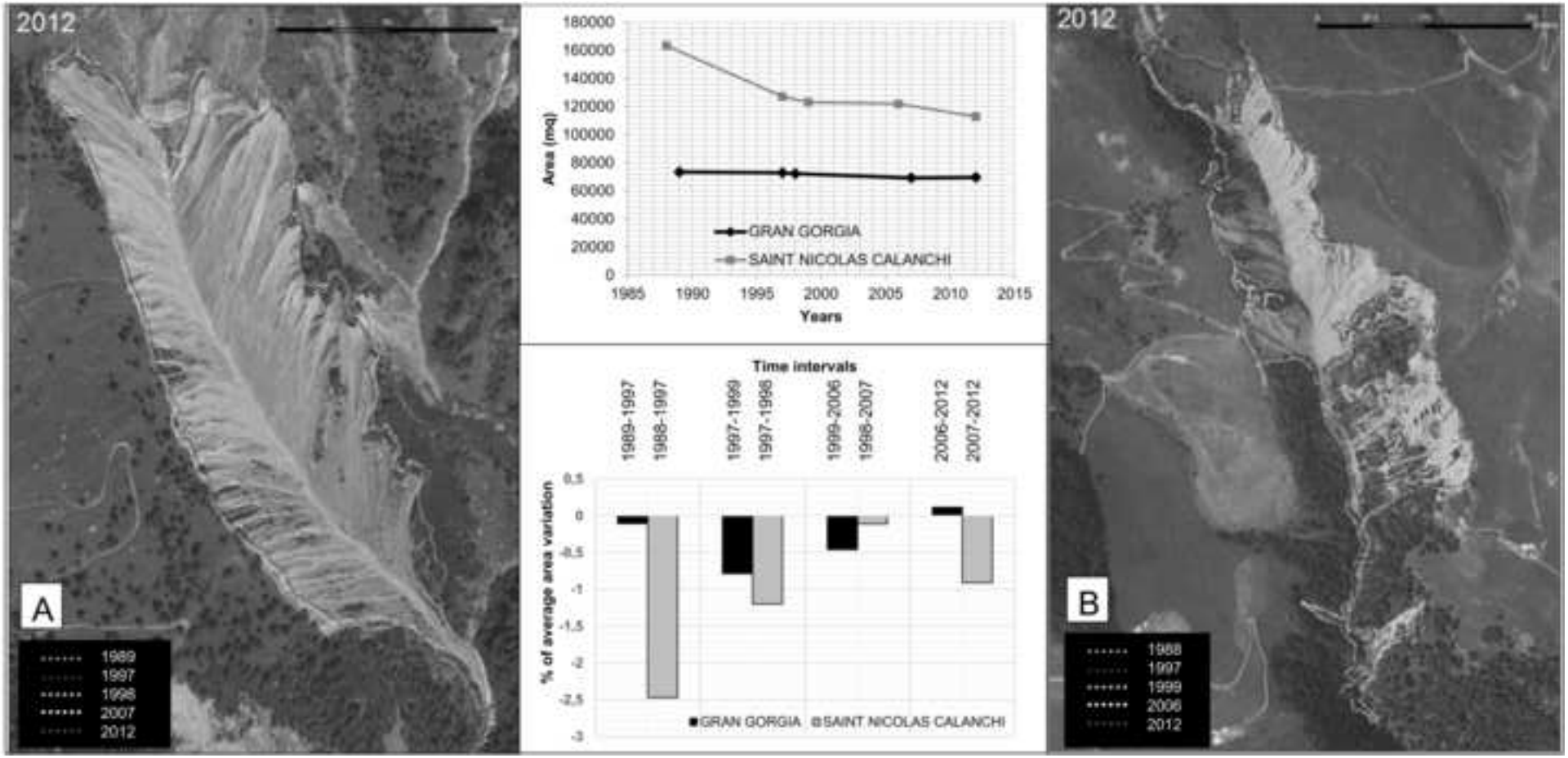

Figure (Greyscale)_5_R1

Click here to download high resolution image

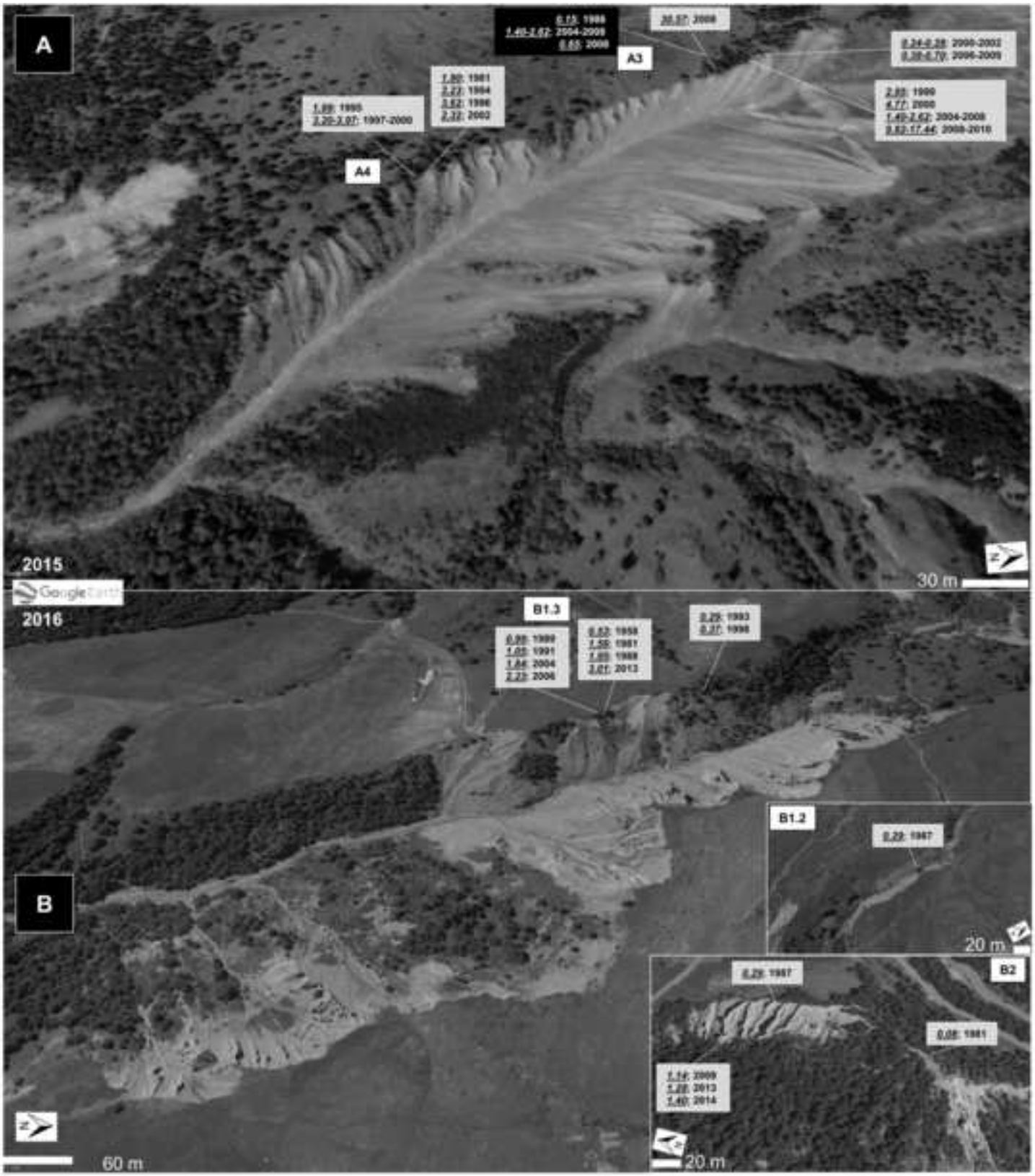

Figure (Greyscale)_6_R2
Click here to download high resolution image

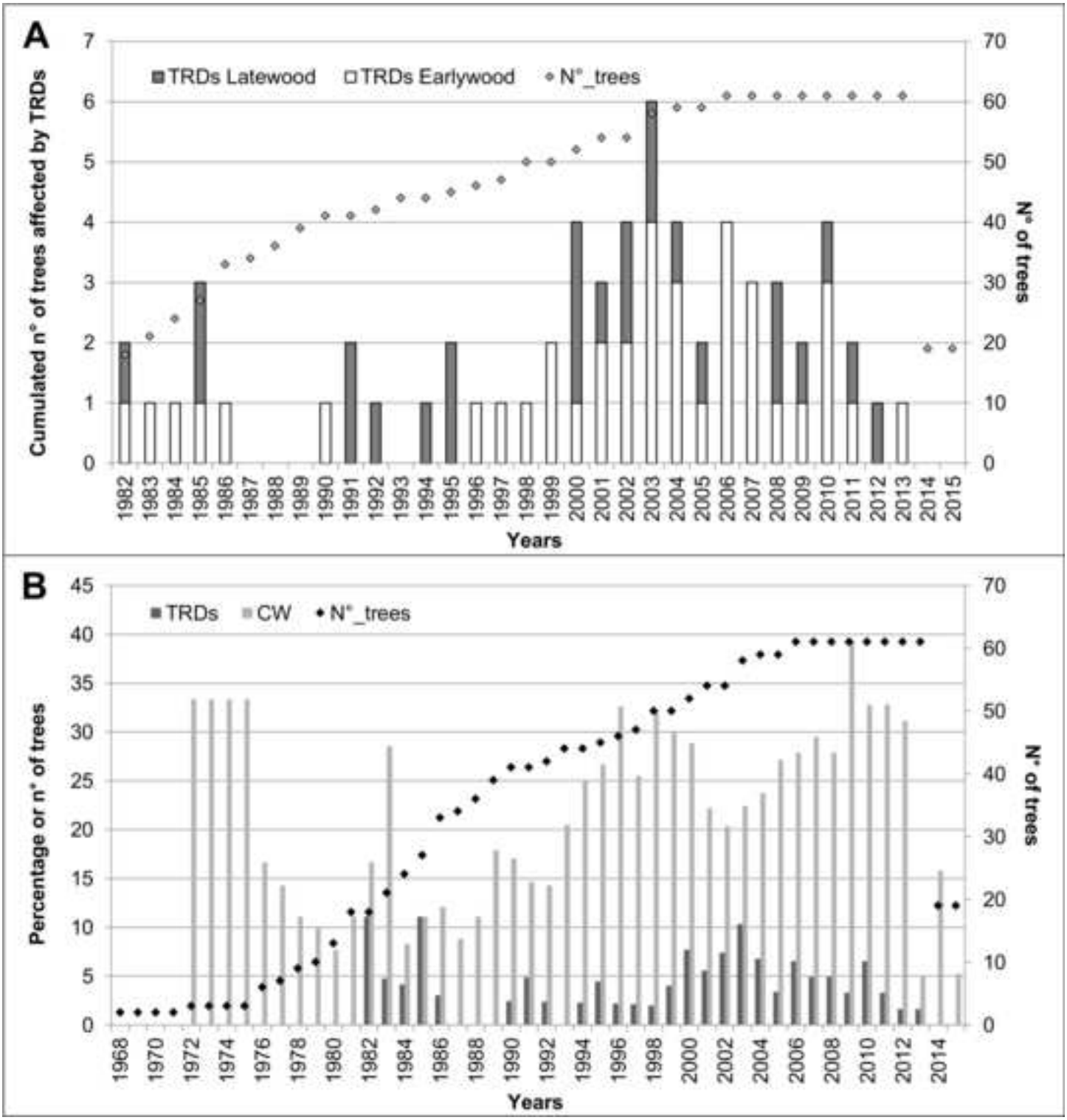

Figure (Greyscale)_7_R1

Click here to download high resolution image

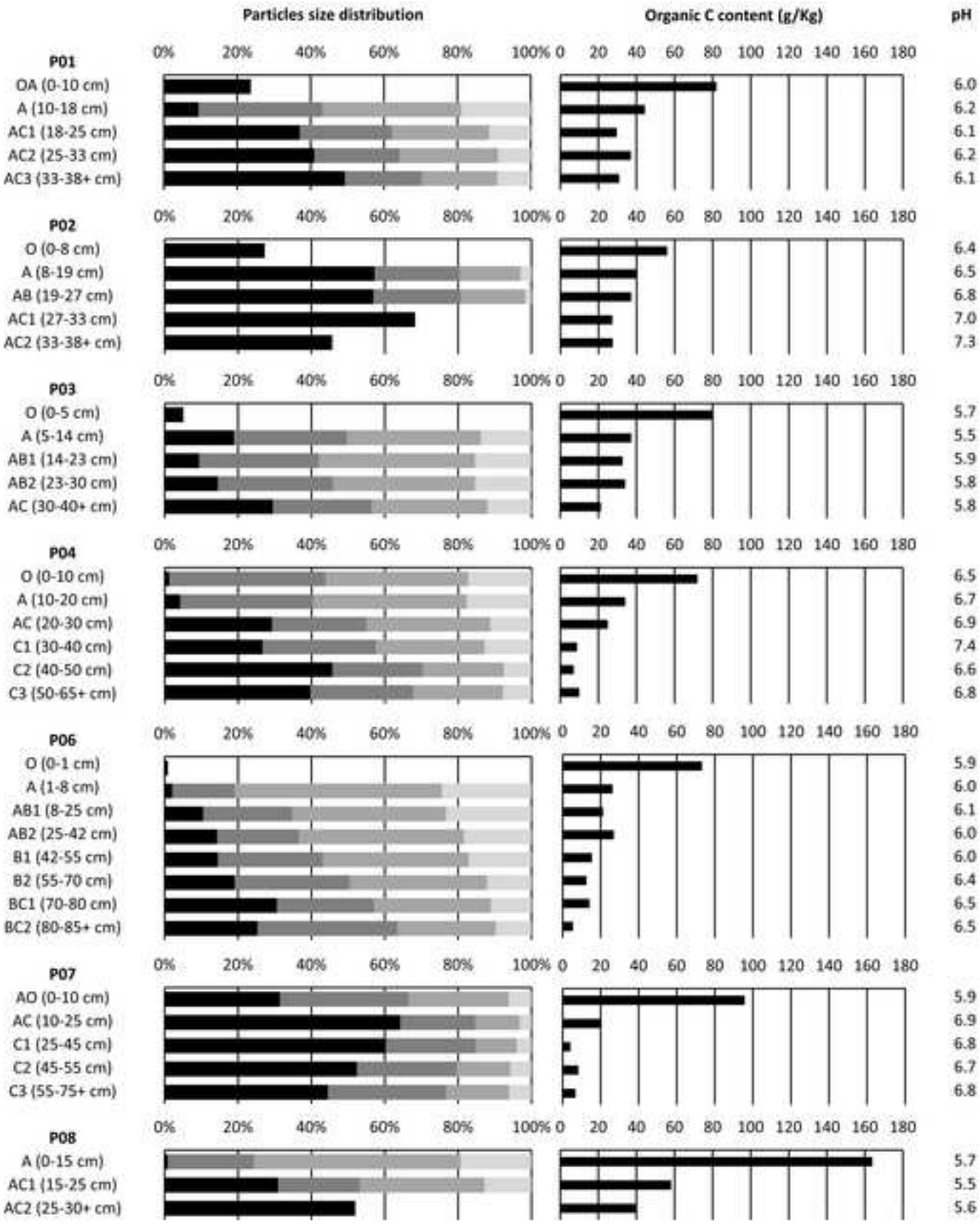

Figure (Greyscale)_8_R1

Click here to download high resolution image

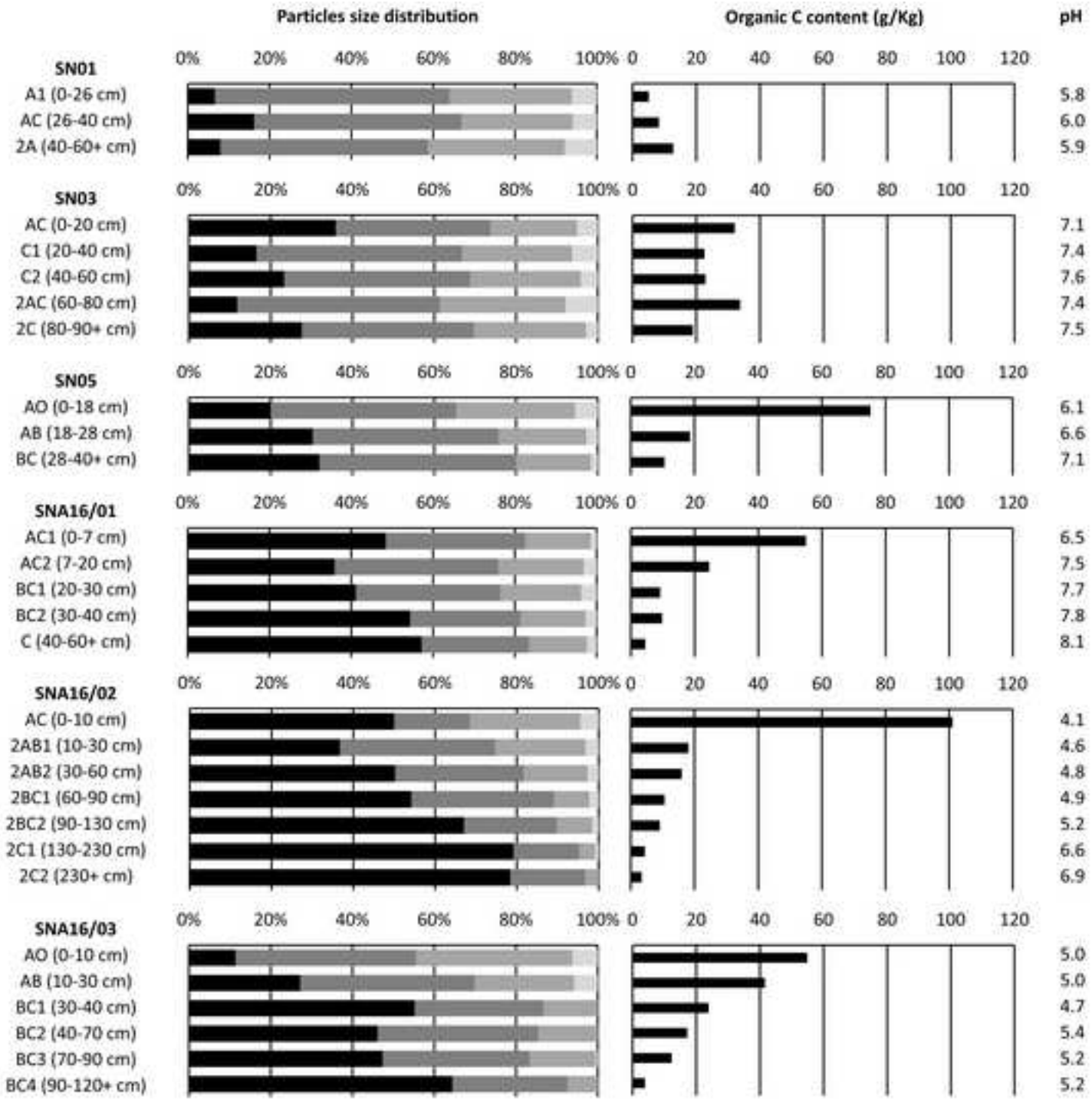

Interactive Map file (.kml or .kmz)_R1

Click here to download Interactive Map file (.kml or .kmz): Study_Sites_Location_R1.kml

Appendix_1

Click here to download Supplementary material for online publication only: Appendix 1.pdf